



Calhoun: The NPS Institutional Archive
DSpace Repository

Theses and Dissertations

1. Thesis and Dissertation Collection, all items

1984

Evaluation of an aerosol prediction model for coastal regions using marine aerosol generation and transport data.

Saunders, David J.

Monterey, California. Naval Postgraduate School

<http://hdl.handle.net/10945/19305>

Downloaded from NPS Archive: Calhoun



Calhoun is the Naval Postgraduate School's public access digital repository for research materials and institutional publications created by the NPS community. Calhoun is named for Professor of Mathematics Guy K. Calhoun, NPS's first appointed -- and published -- scholarly author.

Dudley Knox Library / Naval Postgraduate School
411 Dyer Road / 1 University Circle
Monterey, California USA 93943

<http://www.nps.edu/library>

DOCUMENT KMSO 1000 100
NAME
MAY 11 1943

NAVAL POSTGRADUATE SCHOOL

Monterey, California



THESIS

EVALUATION OF AN AEROSOL PREDICTION MODEL
FOR COASTAL REGIONS USING MARINE
AEROSOL GENERATION AND TRANSPORT DATA

by

David Jesse Saunders

March 1984

Thesis Advisor:

K. L. Davidson

Approved for public release; distribution unlimited

T215685

SECURITY CLASSIFICATION OF THIS PAGE (When Data Entered)

DD FORM 1473
JAN 73

S/N 0102-LF-014-6601

1 SECURITY CLASSIFICATION OF THIS PAGE (When Data Entered)

require a specification of the surface production rate, the entrainment rate (W_s) and the mixed layer depth (h). The model was tested against the data set obtained in the Monterey Bay during the MAGAT 80 experiment. The model was initialized with both observed MAGAT data and an equilibrium initial value, gathered from the JASIN Experiment. The model was run for radii equal to 0.8, 2.0, 5.0 and 10.0 microns. The significance between the observed initial values and the JASIN data is that the MAGAT data was observed from the same air mass as the initial atmospheric data and verification aerosol data. The JASIN initial aerosol data is based on an equilibrium state as a function of only wind speed and reference relative humidity. The model continuously generated a correct gain or loss of aerosol concentrations as defined by the observed MAGAT data, and in most cases the model output is within one order of magnitude of the observed values.

Approved for public release; distribution unlimited.

Evaluation of an Aerosol Prediction Model for Coastal Regions
Using Marine Aerosol Generation And Transport Data

by

David J. Saunders
Captain, United States Air Force
B.S., University of West Florida, 1973

Submitted in partial fulfillment of the
requirements for the degree of

MASTER OF SCIENCE IN METEOROLOGY

from the

NAVAL POSTGRADUATE SCHOOL
March 1984

TABLE OF CONTENTS

I.	INTRODUCTION	9
II.	BACKGROUND	12
	A. DESCRIPTION OF EXISTING MODELS	12
	B. THE NPS BOUNDARY LAYER MODEL	15
	C. MODEL INPUTS AND AEROSOL INITIALIZATION	17
	D. EQUILIBRIUM AEROSOL MODEL	20
III.	DATA ACQUISITION AND SYNOPTIC CONDITIONS	22
	A. DATA ACQUISITION	22
	B. SYNOPTIC DATA	23
	C. SYNOPTIC CONDITIONS	32
	D. DATA SELECTION	33
IV.	MODEL INITIALIZATION AND RESULTS	47
	A. DIGITIZED ATMOSPHERIC SOUNDINGS	47
	B. ADDITIONAL MODEL INPUT AND ADJUSTMENTS TO THE DIGITIZED SOUNDINGS	47
	C. AEROSOL INITIALIZATION PROCEDURES	53
	D. FIRST MODEL RUN RESULTS	55
	E. SECOND MODEL RUN RESULTS	59
	F. SUMMARY OF RESULTS	62
V.	CONCLUSIONS	64
	LIST OF REFERENCES	65
	INITIAL DISTRIBUTION LIST	67

LIST OF TABLES

I.	Initial equilibrium aerosol values	54
II.	Initial observed aerosol values	54

LIST OF FIGURES

2.1	Height dependence of aerosol volume and relative humidity above the ocean	13
2.2	Aerosol volume spectrum at $r=5$ microns as a function of wind speed, U	14
2.3	Profile of (a. Mixed layer and (b. vertical aerosol distribution	16
2.4	Aerosol spectra as a function of size for selected wind speeds	20
3.1	Surface and 500 mb analysis for the western U.S. at 0500 PDT 2, 3 and 4 May 1980	24
3.2	GOES West satellite imagery, 0915 PDT 2 May, 1980	25
3.3	Same as Figure 3.2 except 1245 PDT, 3 May . . .	26
3.4	Same as Figure 3.2 except 1645 PDT, 4 May . . .	27
3.5	Same as Figure 3.1 except 5, 6, and 7 May, 1980	28
3.6	Same as figure 3.2 except 1745 PDT, 5 May . . .	29
3.7	Same as figure 3.2 except 1645 PDT, 6 May . . .	30
3.8	Same as Figure 3.2 except 1745 PDT, 7 May . . .	31
3.9	Plots of wind speed, air and sea surface temperature, and RH beginning 1200 PDT 3 May . .	34
3.10	Same as figure 3.9, except beginning 1800, 6 May	35
3.11	Flight path of aircraft on the morning of 3 May, 1980	36
3.12	Same as figure 3.11 except afternoon of 3 May, 1980	37
3.13	Flight path of aircraft on 4 May 1980	38

3.14	Same as figure 3.13 except 6 May, 1980	39
3.15	Same as figure 3.13 except morning of 7 May 1980	40
3.16	Same as figure 3.13 except afternoon of 7 May 1980	41
3.17	Cruise track of R/V ACANIA 3 May 1980	42
3.18	Same as figure 3.16 except 4 May 1980	43
3.19	Same as figure 3.16 except 6 and 7 May 1980 . . .	44
4.1	Digitized scunding for first model run, 3 May 1980, 1143 PDT	49
4.2	Same as figure 4.2, except for second run, 6 May 1980, 1749 PDT	50
4.3	Plots of inversion and LCL heights, temperature, and humidity profiles, first run	51
4.4	Same as Figure 4.3, except for second run . . .	52
4.5	Aerosol plots for first run, with a) $r = 0.8$ μm , and b) $r = 2.0 \mu\text{m}$	57
4.6	Same as figure 4.5, except a) $r = 5.0 \mu\text{m}$, and b) $r = 10 \mu\text{m}$	58
4.7	Aerosol plots for second run, a) $r = 0.8 \mu\text{m}$, and b) $r = 2.0 \mu\text{m}$	60
4.8	Same as figure 4.7, except a) $r = 5.0 \mu\text{m}$ and b) $r = 10 \mu\text{m}$	61

I. INTRODUCTION

There is an increased emphasis in the ability to forecast the behavior and evolution of aerosols. The scattering and absorption of light are influenced by aerosol distributions in the atmospheric boundary layer and affect the performance of optically guided weapon systems. The Air Force is particularly interested in how aerosol extinction affects the use of precision guided munitions (PGM) [Cottrell et al, 1979]. The Department of Defense (DOD) has PGM's that operate at differing wavelengths which range from the visible to the microwave regions. PGM's have a greater ability to hit a target than conventional munitions; however, the controlling factor is the ability of the guidance system to "see" the target. This ability is dependent on the wavelength for which the sensors are designed and the properties in the intervening atmosphere. The degrading properties in the atmosphere are principally molecular absorption and aerosol scattering. The wavelengths for the guidance systems are designed such that the molecular absorption is minimized: therefore, scattering by aerosols becomes the main concern once a suitable absorption-free window has been selected.

The model under consideration includes the behavior of marine aerosol components as well as previous continental components. Estimating the influences of marine aerosols on electro-optical (EO) systems has been studied [Barnhart and Streete, 1970]. Particle sizes of interest are those associated with locally generated sea salts because of their effects on IR as well as visible wavelengths. The size distributions of sea salt particles show a variance of several orders of magnitude.

The ability to forecast the behavior of aerosol extinction from synoptic scale patterns would help in the deciding which type of weapon system to employ. Because some systems are launched from the air, it is important that such a profile include the vertical distributions of aerosol particles. Models exist for estimating vertical extinction profiles, but they have not been sufficiently verified. To do this, profiles of actual aerosol data must be gathered and compared with the model forecasts.

Models in current use are based on parameterizations of the effects of relative humidity and wind speed on the equilibrium aerosol distributions [Wells, et al, 1977]. Recent evaluations have shown that these models are limited to mean distributions (i.e., the average aerosol concentration at a given wind speed and humidity) [Fairall et al, 1982a]. Models are limited because some processes in the atmospheric mixed layer which affect aerosol concentrations are not considered, namely entrainment and inversion height changes.

The purpose of this study is to present and evaluate a model which includes the meteorological processes that adequately describe the whole marine atmospheric boundary layer (MABL). An inversion represents a cap to the vertical transport of surface generated aerosols, and is not accounted for in previous models. The top of the boundary layer is capped by the marine inversion, where entrainment of overlying air takes place. Because entrainment mixes clear (non-marine) air into the marine layer, this process is as important as surface layer fluxes in determining equilibrium concentration. This entrainment process is included in the model.

Evaluation of the model output will be done with the data from an experiment entitled Marine Aerosol Generation and

Transport (MAGAT). The experiment was conducted in the vicinity of Monterey Bay, Ca, during the period of 28 April to 9 May 1980. The purpose of the experiment was to examine the compatibility of optical and micrometeorological propagation theory, and to extend dynamic models of the evolving MABL to include aerosol and turbulence profiles [Fairall, 1980 and Fairall et al, 1980]. Two platforms, the R/V ACANIA, and an aircraft were used.

In this study, two 24-hour periods were chosen for evaluation; 3 May, beginning at 1200 PDT and 6 May, beginning at 1800 EDT. These periods were chosen because the boundary layer was undisturbed (no fronts closer than 100 nm) for 24 hours prior to the starting times. Additionally, the times were selected due to the proximity of the aircraft and surface ship during the experiment times. The approach was to describe the synoptic conditions from 24 hours in advance of the model forecast through the end of each forecast, and compare the model output with the actual MAGAT findings.

II. BACKGROUND

A. DESCRIPTION OF EXISTING MODELS

Current models for estimating aerosol equilibrium distributions use meteorological inputs of (10-m height) wind speed and relative humidity. These two quantities are considered because of their role in generation and transport (wind) and growth (humidity) of aerosols. The Navy's Wells-Munn-Katz (WMK) [Wells et al, 1977] is an example of this concept. The performance of this type of model has been studied with data obtained in the northern Atlantic and eastern Pacific Ocean areas. The model output compared with these data is shown in figure 2.1, depicting a height dependence of total aerosol volume from a sample set of eastern Pacific data. These profiles correspond to (1) the observed sea salt volume, V ; (2) the observed sea salt volume adjusted to 80% relative humidity, V_0 ; and (3), the WMK predicted volume adjusted to 80% relative humidity (circles). It is clear from this figure that within the mixed layer the observed decrease of aerosol volume with height is less than the model predicts. The surface generated aerosols appear to be well mixed below the inversion when normalized to 80% relative humidity.

The assertion that existing models can predict only a mean value appears in the results obtained in the North Atlantic, from the JASIN Experiment. Figure 2.2 compares a single radius size of five microns and the corresponding model prediction. The values and trends in the predicted and mean results are in reasonable agreement. However, the standard deviation is three times the mean; if one assumes a normal distribution, only 67% of the observed aerosol

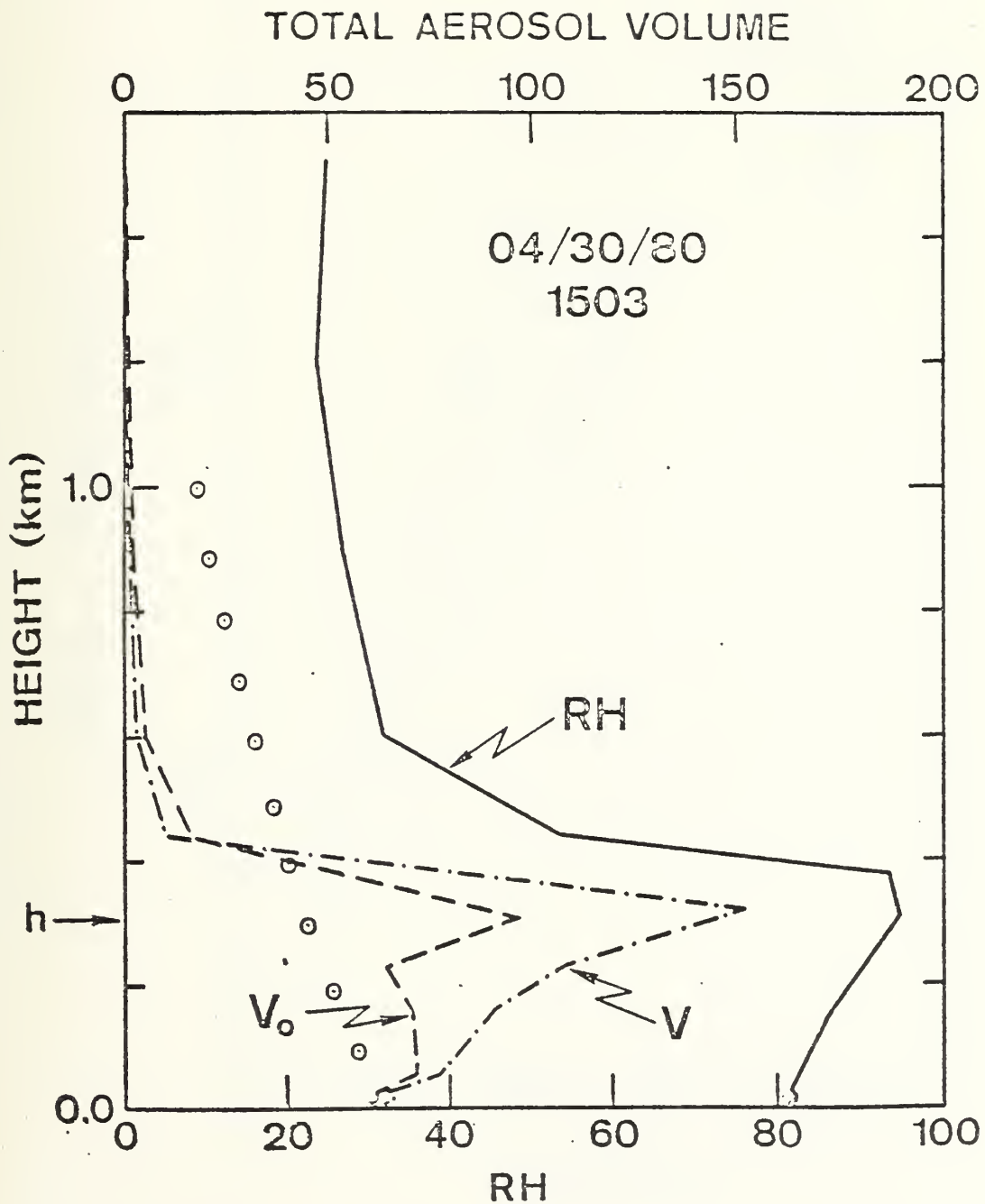


Figure 2.1 Height dependence of aerosol volume and relative humidity above the ocean.

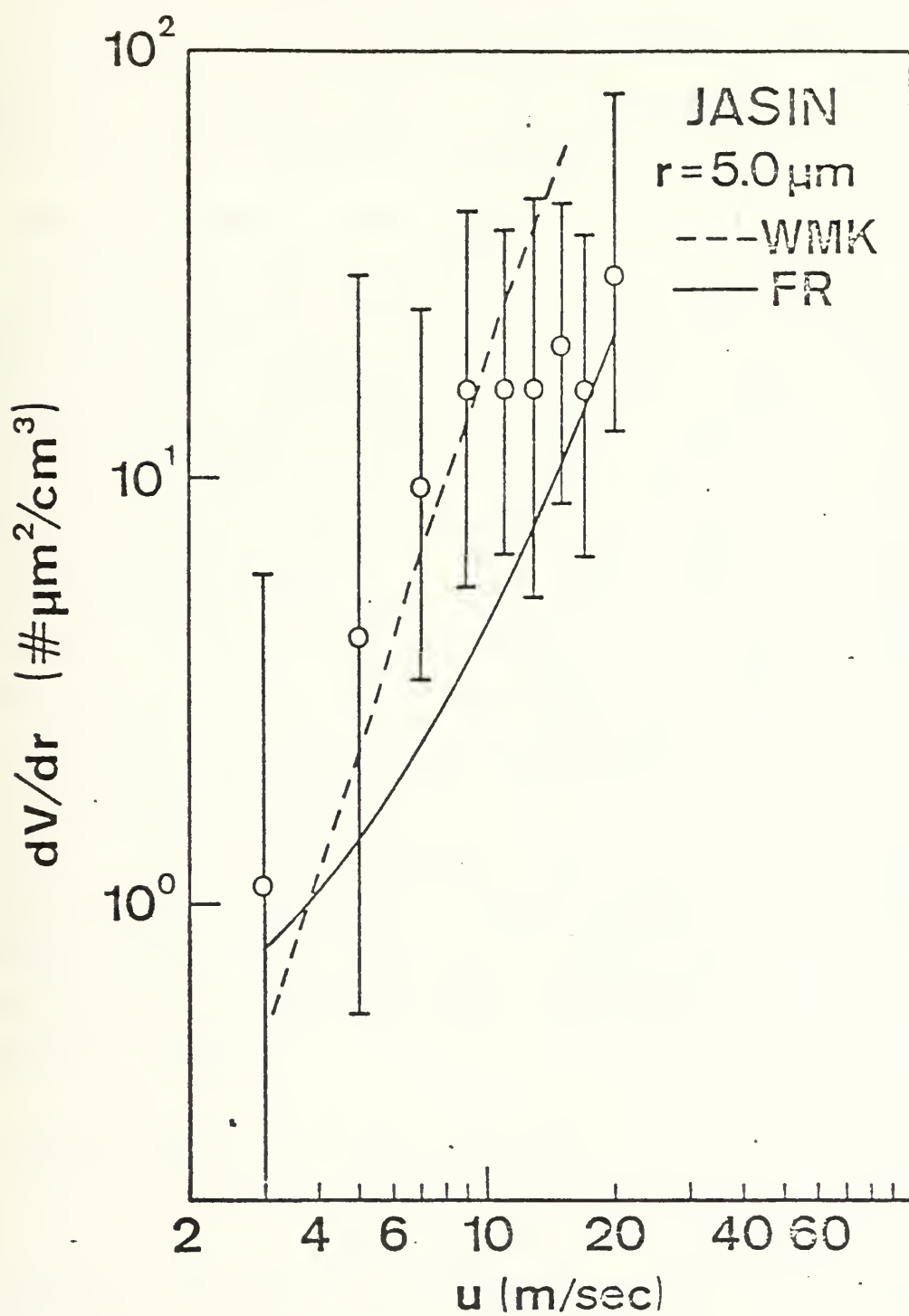


Figure 2.2 Aerosol volume spectrum at $r=5$ microns as a function of wind speed, U .

distributions will be within a factor of three of the average. This comparison emphasizes the point that no matter how accurately a model predicts an average aerosol density at a given wind speed and relative humidity, the factor of three RMS variations cannot be eliminated without considering more meteorological parameters.

E. THE NFS BOUNDARY LAYER MODEL

The distinguishing feature of this model is the characterization of the MAEL, which is convectively mixed up to a height h , and capped by an inversion. The atmospheric profile is depicted in figure 2.3a, representing a cloud-free mixed layer where water vapor mixing ratio (q), and virtual potential temperature (θ_v) are "well-mixed", ie, independent of height in the mixed layer. The assumed vertical aerosol profile is shown in figure 2.3b. The model produces a 24-hour time evolution of an aerosol spectrum, requiring a prediction of the following at each time step:

- 1) surface production rate of marine aerosols
- 2) entrainment rate at the top of the mixed layer
- 3) mixed layer depth.

Details of how these parameters are input into the model are discussed in chapter IV. The mathematical relationship between the time rate of change of the aerosol volume spectrum, dv/dr , and these three parameters is shown in the following equation

$$\frac{dv}{dt} = \underset{1}{(\langle w'v' \rangle_o)} - \underset{2}{(w_e + w_{km})} \underset{3}{v} / h \quad (2.1)$$

The model predicts the evolution of aerosol at five radii (0.8, 2.0, 5.0, 10.0, and 15.0 microns) of both the continental and the marine (sea salt) components in the mixed

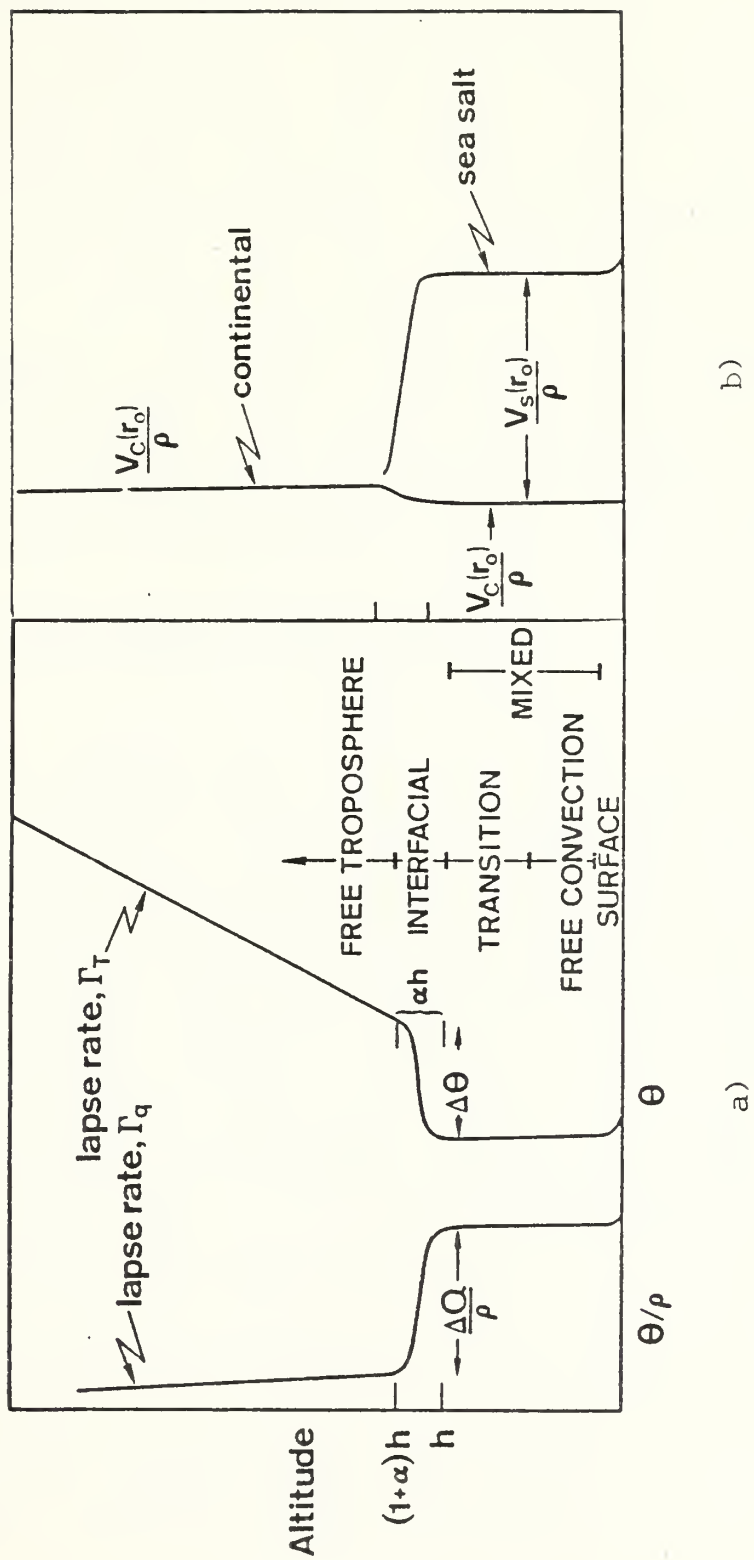


Figure 2.3 Profile of a) Mixed layer and
b) vertical aerosol distribution.

layer. The actual time evolution of each radius is output in the form of dv/dr , with the units of $\mu m^2 / cm^3$.

The model assumes no appreciable concentration of marine aerosols above the mixed layer. The entrainment of air into the mixed layer will not cause an element of these marine particles to "escape" into the free troposphere. The ocean acts as a source for marine aerosols, primarily through the generation of white caps. This is the only input for the marine component. The ocean also acts as a sink for the continental aerosols, which are generally of a smaller radius. The entrainment process at the top of the mixed layer mixes clear (non-marine) air into the MABL. This process could be as important as the surface layer fluxes in determining an aerosol concentration.

C. MODEL INPUTS AND AEROSOL INITIALIZATION

The model is designed so that with the exception of initializing the aerosols, all of the calculated parameters are based on inputs from surface based observations, and representative soundings. The input consists of:

- 1) Non-meteorological inputs of latitude, julian day, and the local start time. These are used for a diurnal radiative heating/cooling package. Diabatic warming has an obvious impact on the life and strength of the mixed layer. Additionally, sea-surface temperature (SST) is input at the start time. Up to ten forecast SST values can be input during the 24-hour period as well.
- 2) Surface wind speed and direction at the start time and, as with SST, up to ten additional forecast values.
- 3) From figure 2.3, temperature and relative humidity are parameterized by virtual potential temperature and water

vapcr mixing ratio, respectively. Mixing ratios are input above the mixed layer, as well as the lapse rate above the "jump".

An initialization of the six radii concentrations in three regimes is required. To do this it is necessary to understand the actual distributions of the continental and marine components in the mixed layer. For the purposes of evaluating the model, assumptions must be made on the distributions of the acquired MAGAT data. The aircraft instruments could not distinguish the chemical make-up of the individual particulates; therefore, it is not known, for a given radii concentration in the mixed layer, how much is continental and how much is marine. The concentrations of each size were calculated in the mixed layer, and then above the mixed layer. Based on the assumption that there are no marine concentrations above the mixed layer, we conclude that the concentrations calculated from above are all continental, and therefore linearly subtracted from the concentrations in the mixed layer, leaving only marine concentrations.

A further adjustment of the input aerosol values is required, based on changes in relative humidity during the data collection time. We have stated that the growth of aerosols is a function of relative humidity. Therefore, a distribution of aerosols gathered at 90% humidity cannot be directly compared to another distribution gathered at 80 % humidity; a reference humidity is required. Consider the aerosol volume spectrum

$$v(r) = 4/3 \pi r^3 n(r) \quad (2.2)$$

where $n(r)$ is the number density spectrum. $V(r)$ is defined as the volume of aerosol particles per cm^3 at a reference saturation ratio of $S=80\%$. A humidity growth factor $G(S)$ [Fairall, et al, 1982a] is defined as

$$G(S) = .81 \exp(.066S/(1.58-S)) \quad (2.3)$$

There are further considerations concerning advection. Clearly all aerosols do not originate locally; both above and below the inversion aerosols are advected into a local region. In terms of aerosol density, entrainment acts as an aerosol flux out of the boundary layer because the concentrations above and below the layer are different. In the model, the entrainment acts on the "jump" across the inversion. For the purpose of evaluating the evolution of a local concentration of aerosols, the model will neglect horizontal advection and further assume a negligible local production of the continental component. The model takes into consideration a Stokes gravitational fallout term, W_k [Wu, 1979]. The fallout rates above and below the inversion are different because of the change in aerosol spectra, caused by the humidity growth factor. The Stokes velocity [Fairall, et al, 1982a] is calculated from the following equation where ρ_w is the density of the droplet and E is the kinematic viscosity of the air.

$$W_k = 2g(\rho_w - \rho)r^2G^2(S)/(9E\rho) \quad (2.4)$$

D. EQUILIBRIUM AEROSOL MODEL

As a means of comparison of aerosol initialization schemes, the model offers the option of initialization with equilibrium values. These initial values are based on data collected from the JASIN Experiment [Fairall, et al, 1982]. A large aerosol data base was collected during equilibrium conditions, with respect to wind speed, during 12 hour periods and then normalized to a reference relative humidity. Aerosol spectra were then grouped into six different wind speed ranges. For the equilibrium initialization scheme in the NFS model, a pre-assigned value of the five radii are used as initial aerosol values, based on the wind speed at the model start time. An example of the equilibrium aerosol spectra from the JASIN Experiment is shown in figure 2.4. Note that the reference relative humidity for this experiment was 87 percent. The graph is referenced here only to show an equilibrium type distribution; the initial equilibrium and MAGAT aerosol values will be shown in chapter IV. Once initialized with either equilibrium data or calculated data, the model will run in the same manner.

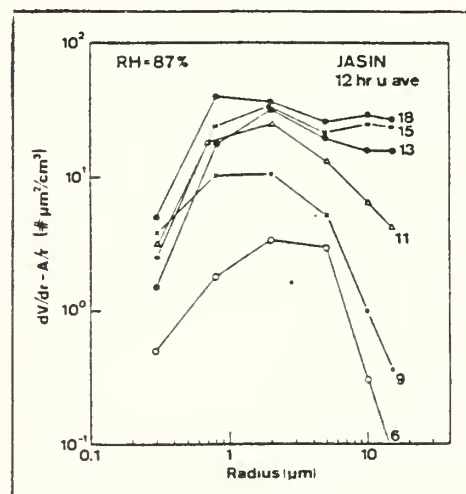


Figure 2.4 Aerosol spectra as a function of size for selected wind speeds.

This equilibrium scheme illustrates the fundamental difference between the NPS model, which is a dynamic model, and a steady-state type model. A representative model using this equilibrium approach is the WMK model, mentioned in the beginning of this chapter. This type of output describes the marine aerosol distributions as a function of wind speed (surface generation), relative humidity (growth factor), and elevation (vertical variation of aerosols with height assuming a steady state vertical transport process). The mathematical representation of this model [Fairall, et al, 1982a] is

$$n(r) = (r/a) \cdot 1.62 (C_1 + C_2 v^\delta) F \cdot \exp \left(-z/h_0 F - 8.5 (r/a)^\gamma \right) \quad (2.5)$$

where

r = the particle size in microns,

u = the wind speed,

$v = 0.5$ for $u \leq 4$ m/s,

$v = u - 3.5$ for $u > 4$ m/s,

$f = 1 + (v/60)^3$,

$\gamma = 0.384 - 0.00293 v^{1.25}$,

Z = height above sea surface, m,

h = scale height, m (800 m for $Z < 1000$ m),

$a = 0.81 \exp (0.066s / (1.058 - s))$,

$S = H/100$, (H = relative humidity in percent).

The other constants are given, based on the value of v .

v , m/s	C_1	C_2	δ
$v \leq 7$	350	1000	1.15
$v > 7$	0	6900	0.29

The equation described produces a number density spectrum, $n(r)$. This relates to the volume spectrum $V(r)$, as shown in equation 2.2.

III. DATA ACQUISITION AND SYNOPTIC CONDITIONS

A. DATA ACQUISITION

The data were obtained from a ship and aircraft experiment, Marine Aerosol Generation and Transport (MAGAT), held from 28 April to 9 May 1980, in a region 30 to 50 miles off the coast of Monterey Bay, Ca. Data gathering was done with instruments mounted on both an aircraft and a surface ship, the R/V ACANIA. Aerosol data were obtained from the Airborne Research Associates turbo-charged Bellanca, using a Particle Measuring System (PMS) Axial Symmetric Scattering Aerosol Probe (ASSAP) particle counter. All measured data were sampled every 2.5 seconds, with a two-scan average of every five seconds. The scans were collected in "ladder" profiles, during which the aircraft made measurements at a constant altitude for two minutes, climbed to a new altitude, and repeated a new measurement run. The instrument utilized 60 size channels from 2.8 to 14.0 micron radius. In most cases the ladders extended from near the sea surface (3 m) up through the well-mixed boundary layer, to a few steps above the inversion. The elevation was generally up to 5 kilometers. A typical ladder profile contains 10 to 14 steps. The step heights were randomly chosen, but an attempt was made to keep each step height consistent between ladders. Air and dew-point temperatures were also measured and used to calculate relative humidity for the correction factor mentioned in chapter two. The aircraft also flew ascending spirals (in the vicinity of the ladders) during which other meteorological parameters were collected. This data yielded vertical soundings similar to those provided by radiosondes.

There were two aerosol instruments fitted on the R/V ACANIA. One was the PMS model CSAS (classical scattering) and the other was model ASAS (active scattering), controlled by a PMS data acquisition system (DAS-32) with a computer interface. The shipboard system measured aerosols in 90 different size channels from 0.9 to 14.0 micron radius.

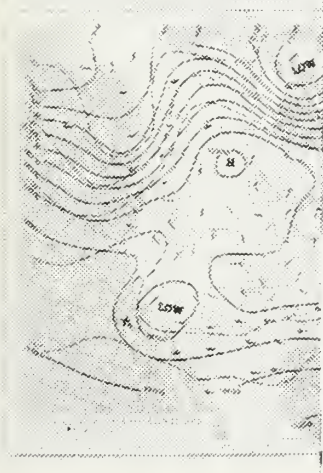
It was noted, during the flybys over the R/V ACANIA, that the aircraft measurements did not agree with that of the ship. The size distributions from the aircraft measurements were consistently smaller than the ship measurements, for radii greater than 1.0 micron. In addition, the differences increased with radius. Since the shipboard aerosol system is newer and had a wider size range, and better sensitivity, aircraft aerosol data were corrected to agree with the ship aerosol data [Fairall, 1980 and Fairall et al, 1980] .

Profiles of virtual potential temperature and mixing ratio were obtained from three different sources. The reason for using these parameters instead of temperature and dew point, is that mixed layer inversions are more easily identified with the former variables. The sources were the spiral flights from the aircraft, the radiosonde launches from NPS and from the R/V ACANIA.

E. SYNOPTIC DATA

Surface and 500 mb synoptic charts and the GOES WEST satellite images were used to evaluate the synoptic conditions. Charts are from the NOAA weekly series of daily weather maps. In addition to data collected from the R/V ACANIA and the aircraft, local weather data were also available from the U.S. Army's Fritzsche Field weather facility,

FRIDAY, MAY 2, 1980



SUNDAY, MAY 4, 1980

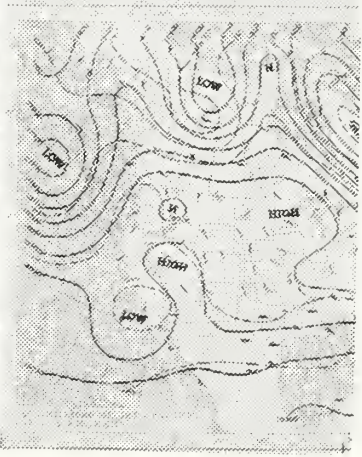
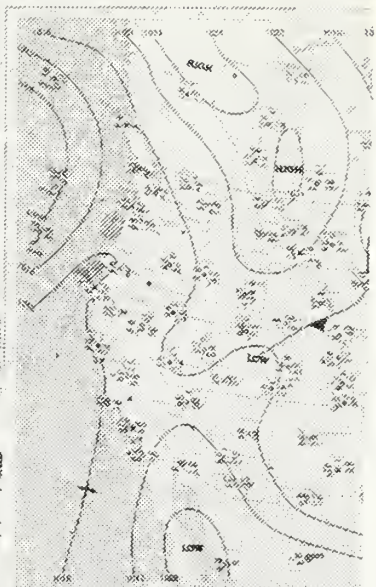
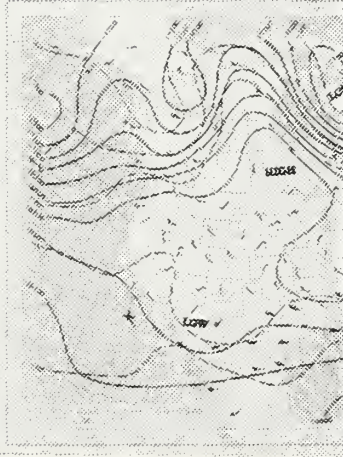


Figure 3.1 Surface and 500 mb analysis for the western U.S. at 0500 PDT 2, 3 and 4 May 1980.

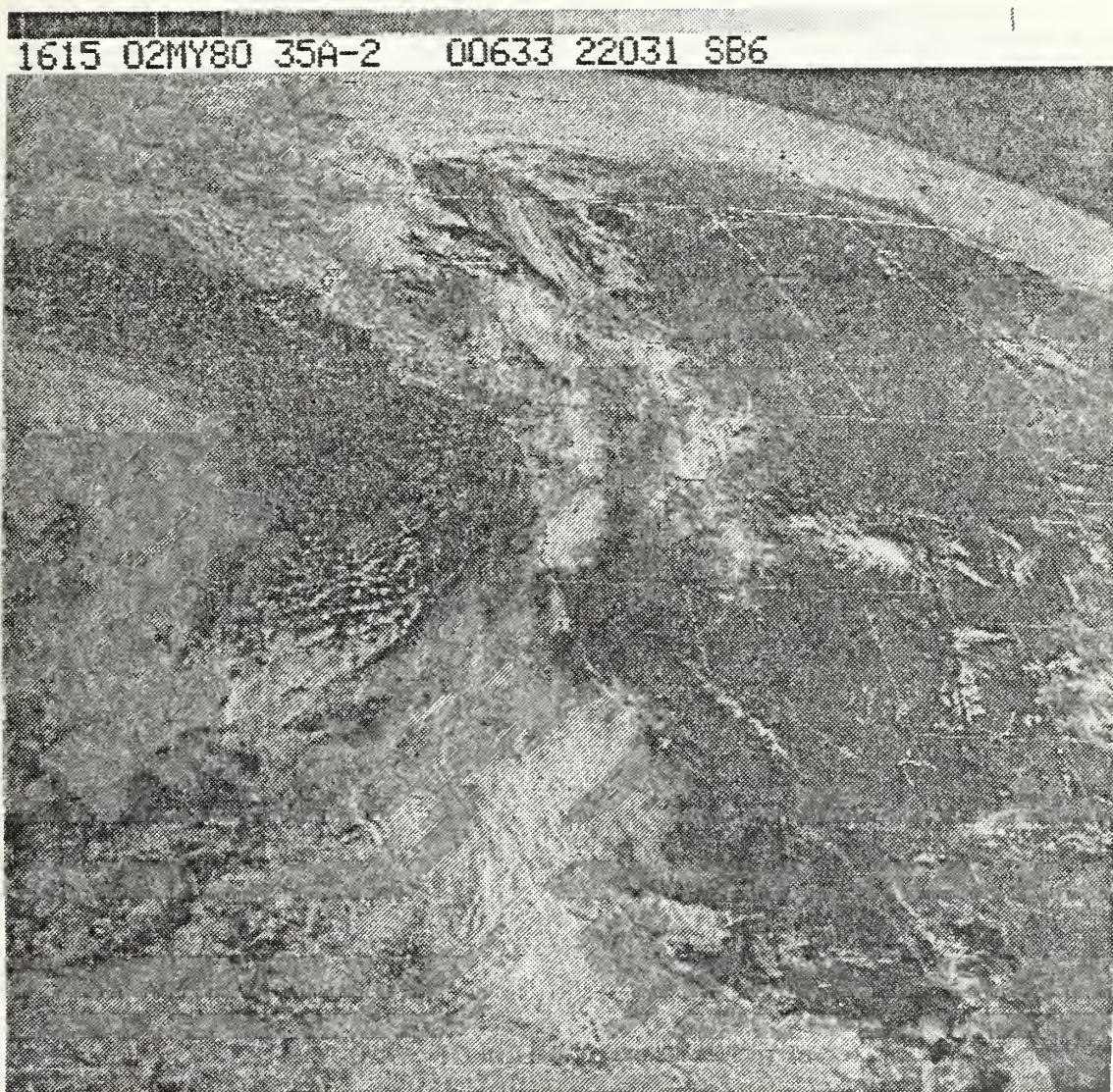


Figure 3.2 GOES West satellite imagery, 0915 PDT 2 May, 1980.

1745 03MY80 35A-4 00362 19161 UC2



Figure 3.3 Same as Figure 3.2 except 1245 PDT, 3 May.



Figure 3.4 Same as Figure 3.2 except 1645 PDT, 4 May.

SUNDAY, MAY 5, 1980

WEDNESDAY, MAY 7, 1980

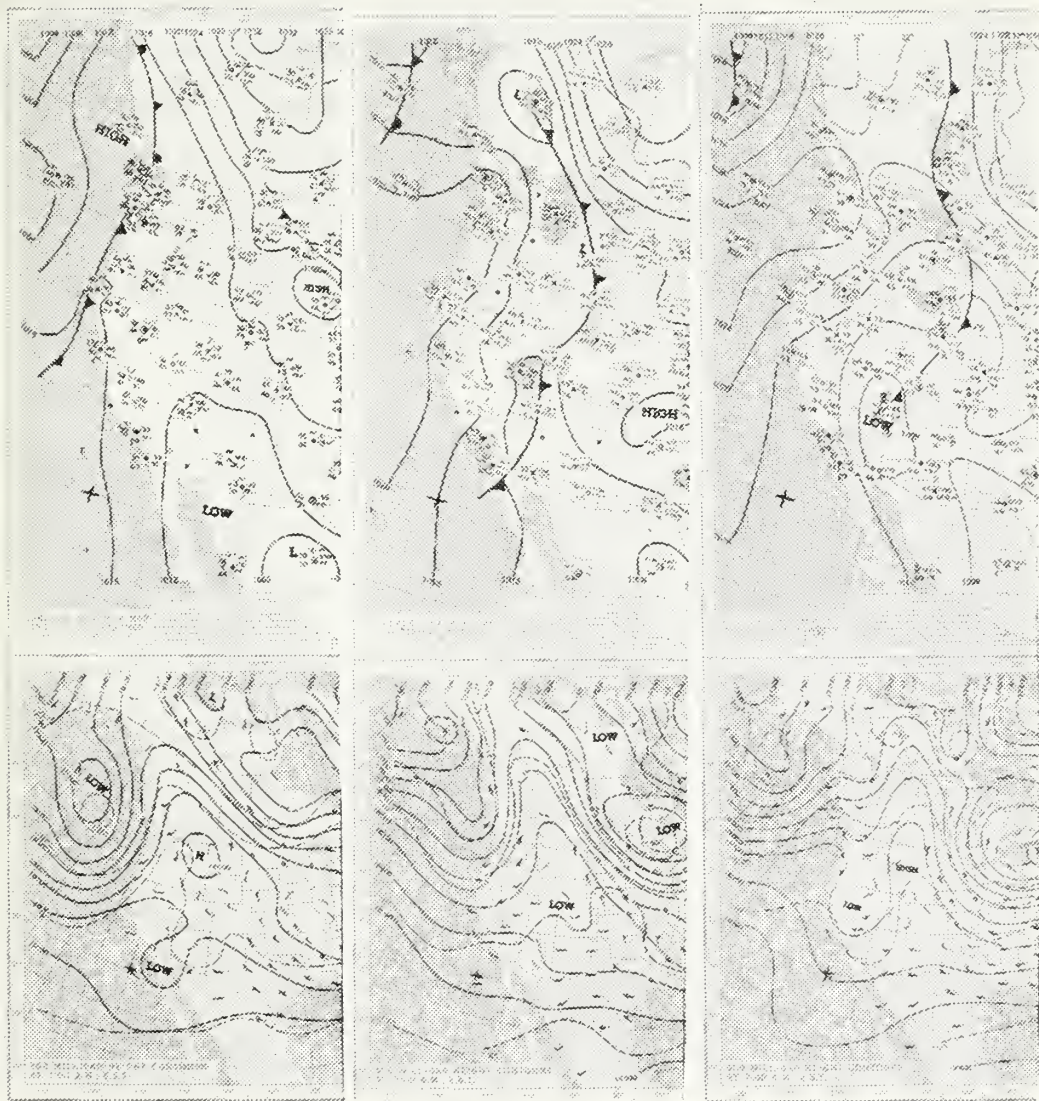


Figure 3.5 Same as Figure 3.1 except 5, 6, and 7 May, 1980.

2345 05MY80 25A-4 00342 19171 UC2

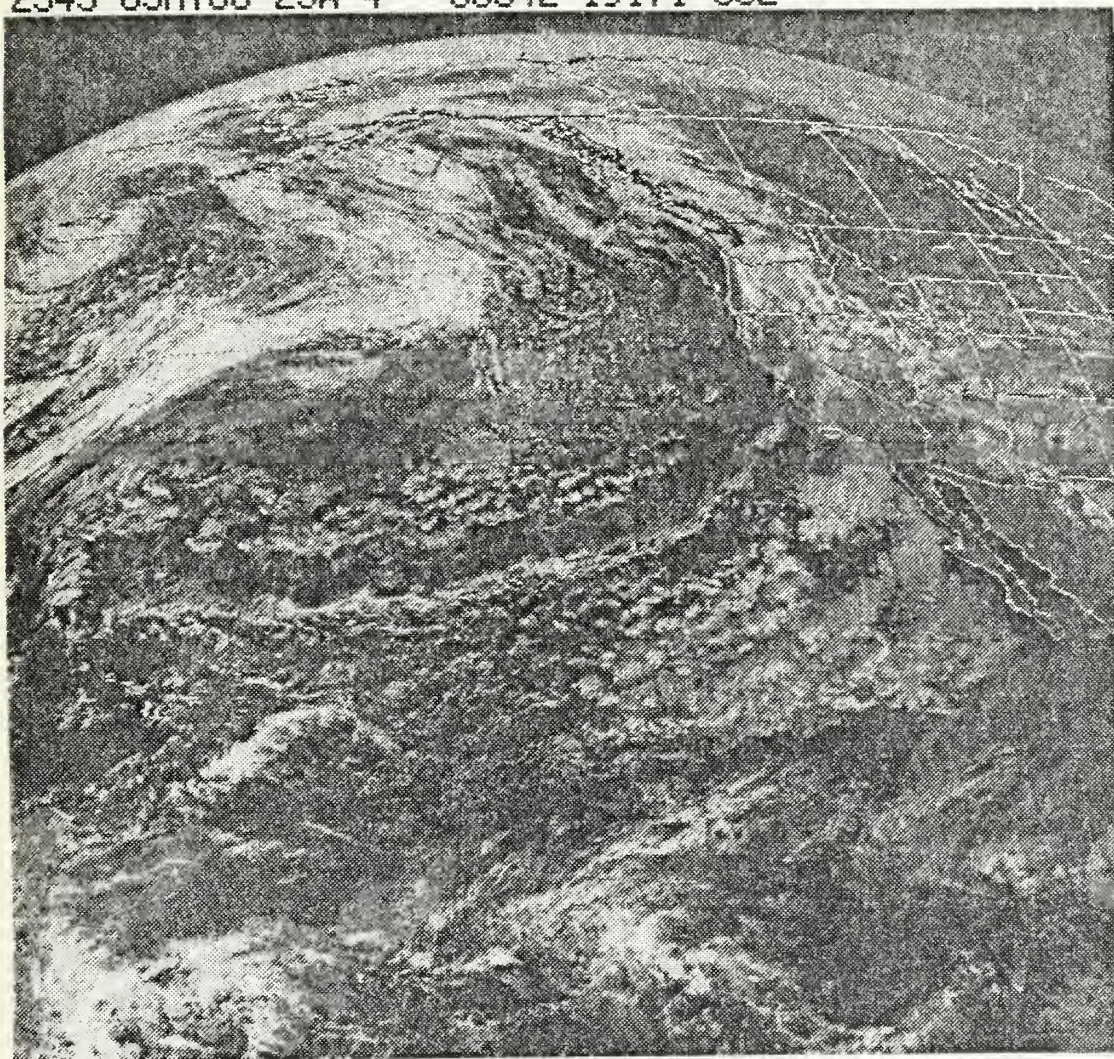


Figure 3.6 Same as figure 3.2 except 1745 PDT, 5 May.

2245 06MY80 35A-4 00342 19171 UC2



Figure 3.7 Same as figure 3.2 except 1645 PDT, 6 May.

2345 07MY80 35A-4 00342 19181 UC2

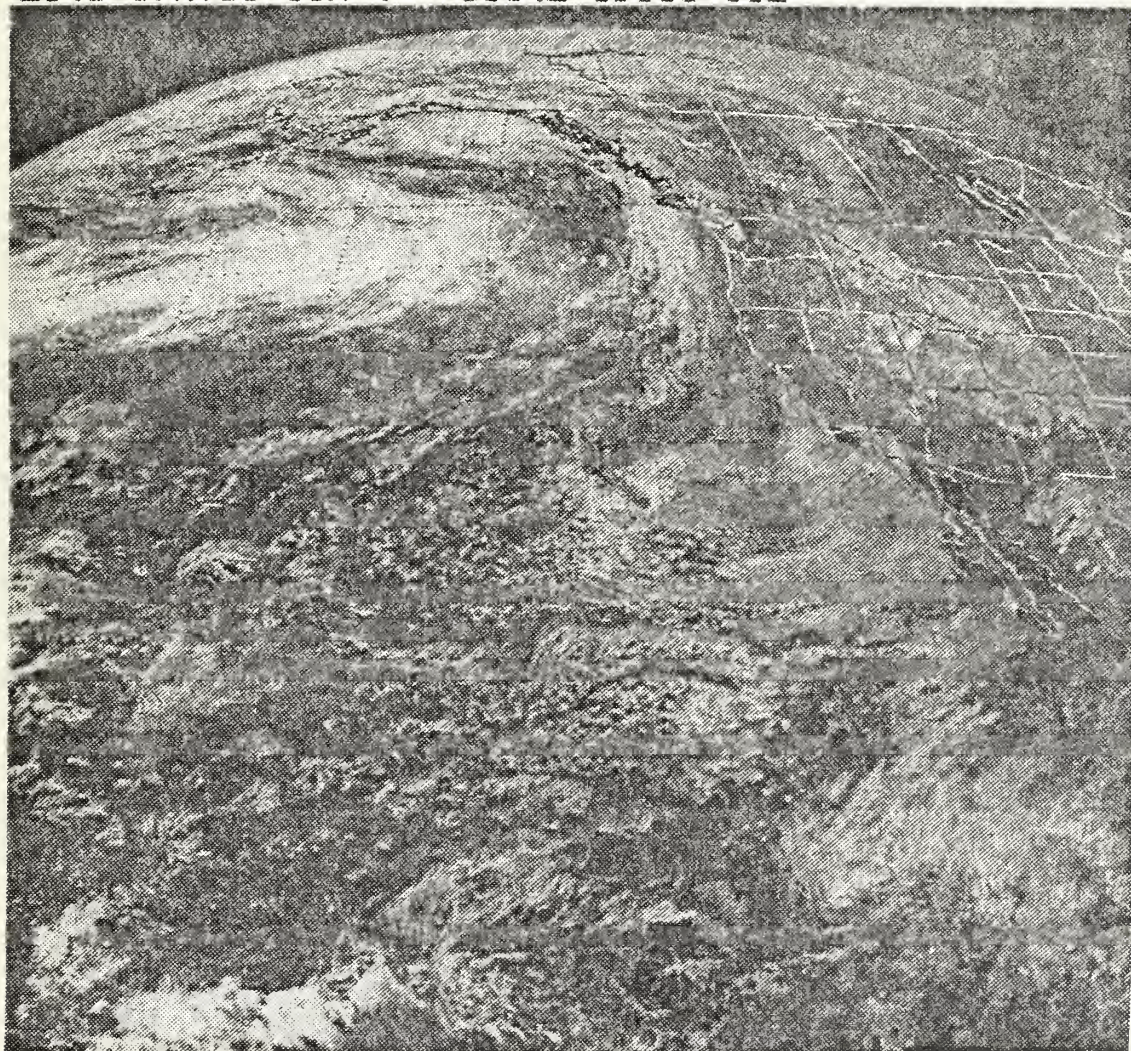


Figure 3.8 Same as Figure 3.2 except 1745 PDT, 7 May.

Fort Crd, Ca. Satellite photographs and NOAA maps for the two different time periods (2-4 May and 6-7 May) are shown in figures 3.1 through 3.8. Each three-day sequence depicts the 24 hour period being considered; 24 hours before and after. Atmospheric soundings for the two model runs are shown in chapter IV, figures 4.1 and 4.2.

C. SYNOPTIC CONDITIONS

Several weak frontal systems passed through the area during the experiment. Showers occurred during the first and last days, associated with the fronts. Low cloudiness and fog occurred during the morning from 29 April to 5 May, with fog returning again on the last day.

At the beginning of the period, the area was dominated by a slowly eastward migration of a cut-off low at 500 mb. By early morning on 2 May, the area was under the influence of a weak ridge. On 3 May the area was under divergent flow at the upper level. An upper level low had formed off the Baja Ca. coast on 4 May, leaving the area under the influence of a col. On 5 May the area was between an upper-level trough and ridge, and by 6 May the area was on the back side of the trough. Because of the deepening of the trough, the area was still on the back side of the trough on 7 May. A new upper level trough formed and approached the area on the final two days of the experiment.

Surface winds were relatively light, 0 to 10 kts, at the beginning of the period, and increased toward the end of the period to 16 kts, gusting to 22 kts.

An important feature of these interpretations is the nature of the mixed-layer, often topped by an inversion, with regard to stability, and therefore mixing intensities. It is assumed that the mixing becomes greater as conditions become more unstable.

At the start of the experiment, the mixed layer exhibited stable to slightly unstable conditions, until about 1800 local time (PDT) 28 April, when conditions became more neutral. The neutral condition remains until 1 May when conditions once again become stable. A weak frontal passage before 0500 PDT on 29 April does not appear to affect the mixed layer profile. The layer remains stable until a frontal passage on 2 May when conditions become neutral and remains so until 5 May. On the morning of 5 May, conditions are slightly stable, but returned to neutral on 6 May, despite a frontal passage at 1300 PDT on 5 May, and remaining neutral to the end of the experiment on 9 May.

D. DATA SELECTION

Data from the MAGAT experiment were selected for model verification on the basis of the relative positions of the two data gathering platforms and the general synoptic conditions. The locations of the surface ship and the aircraft did not always coincide during the experiment. Therefore soundings and aerosol data were considered suitable if the two were within 20 nautical miles. Hourly wind speed, direction, and SST were gathered from the ACANIA and were used along with the aircraft soundings. Plots of wind speed, air (solid line) and sea-surface (dashed line) temperature, and relative humidity for the two 24 hour periods are shown in figures 3.9 and 3.10. Another consideration of the aircraft data was the relative locations of the aerosol ladders and the soundings. Although both gathered during vertical flight profiles, they were not done at the same time. The synoptic conditions during the experiment include periods of frontal weather which was also avoided in the analysis. Two time blocks

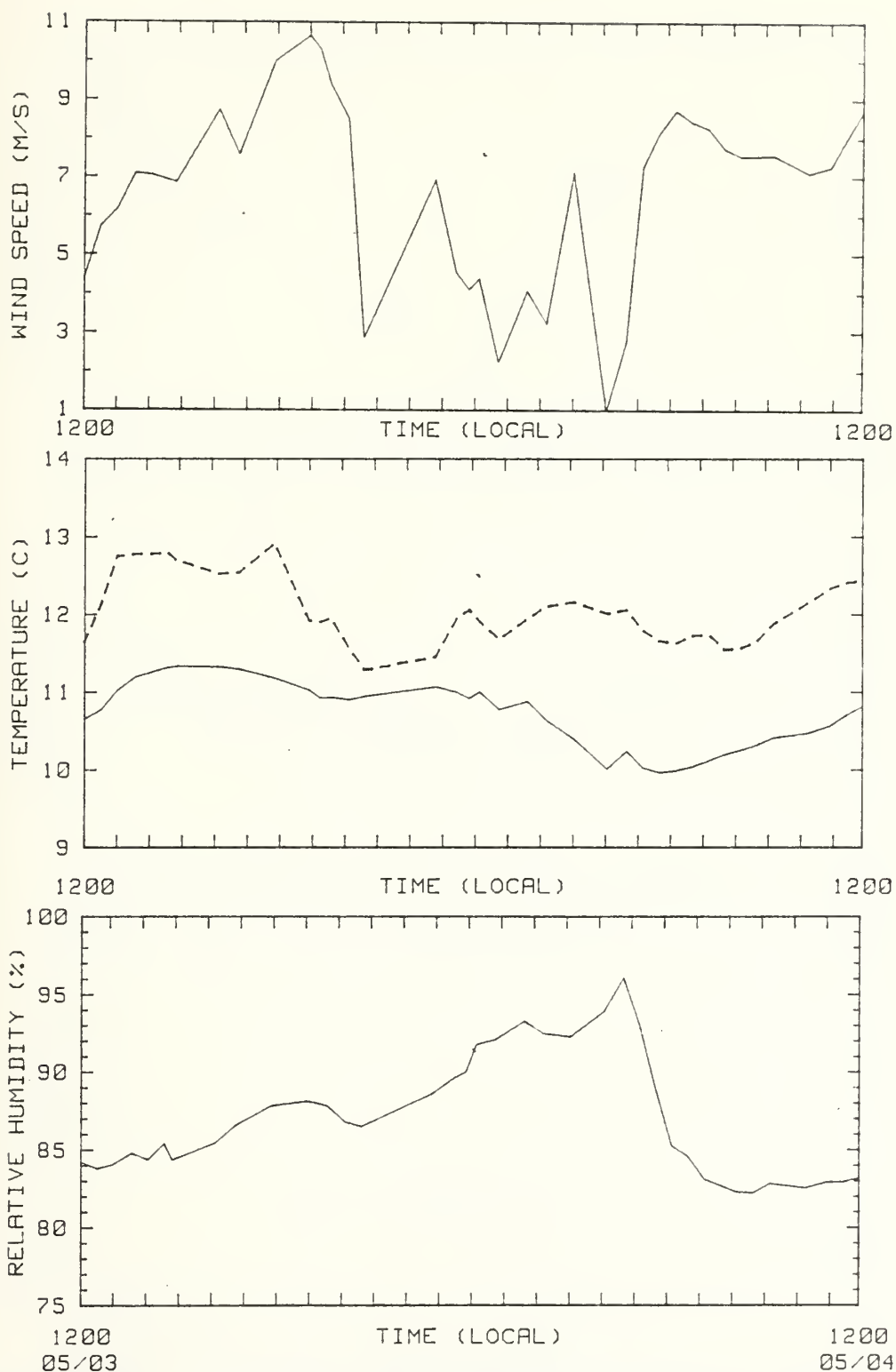


Figure 3.9 Plots of wind speed, air and sea surface temperature, and RH beginning 1200 PDT 3 May.

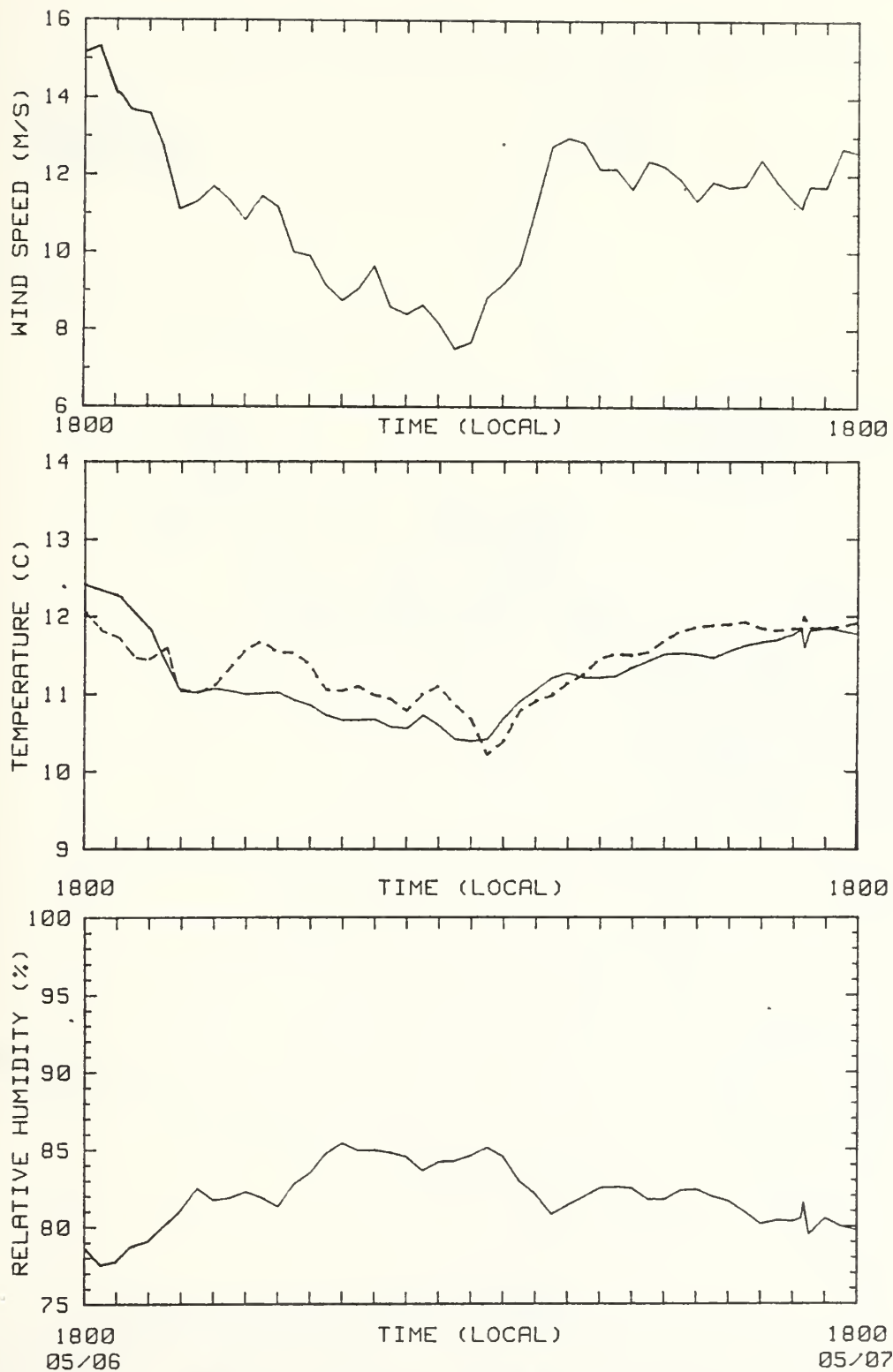


Figure 3.10 Same as figure 3.9, except beginning 1800, 6 May.

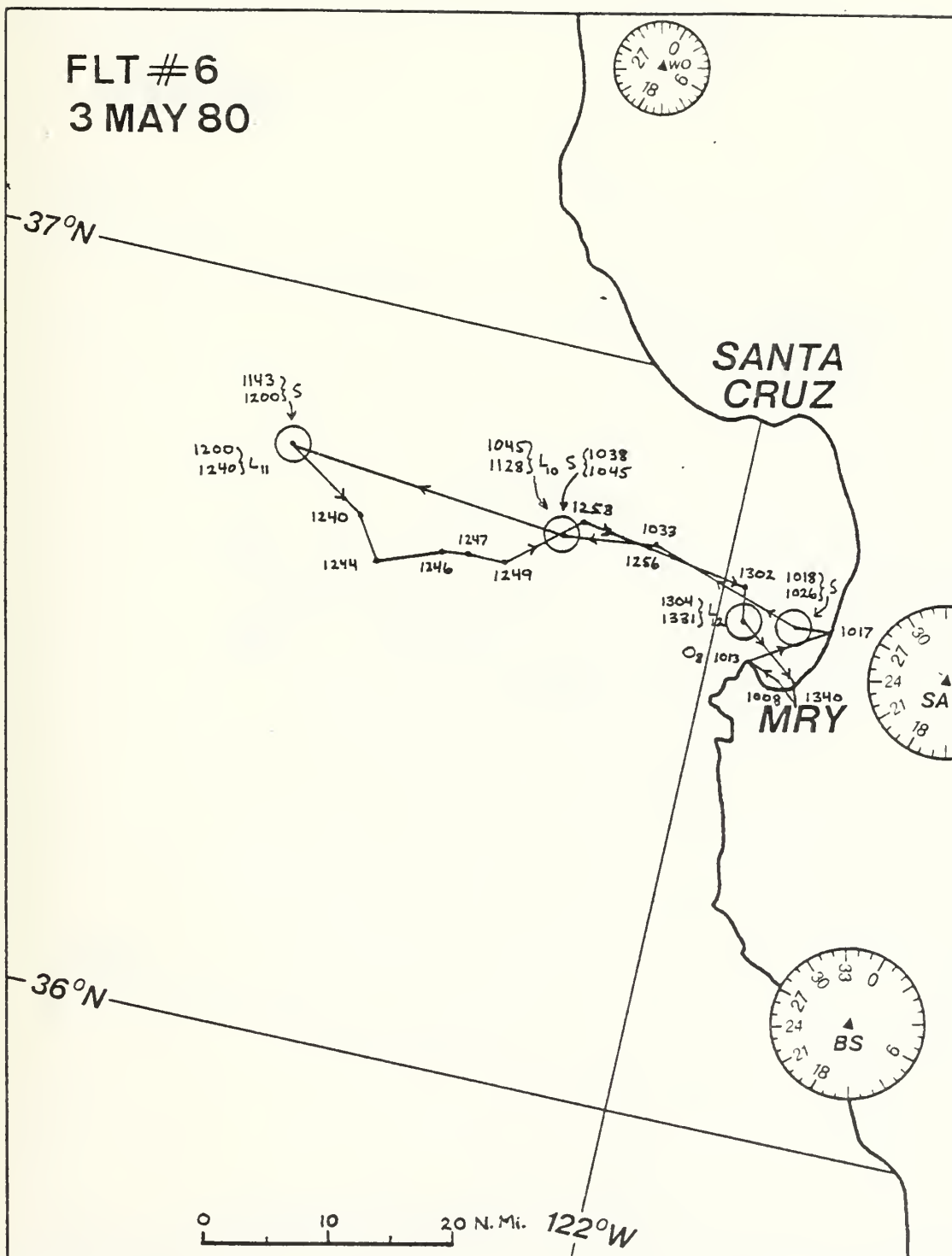


Figure 3.11 Flight path of aircraft on the morning of 3 May, 1980.

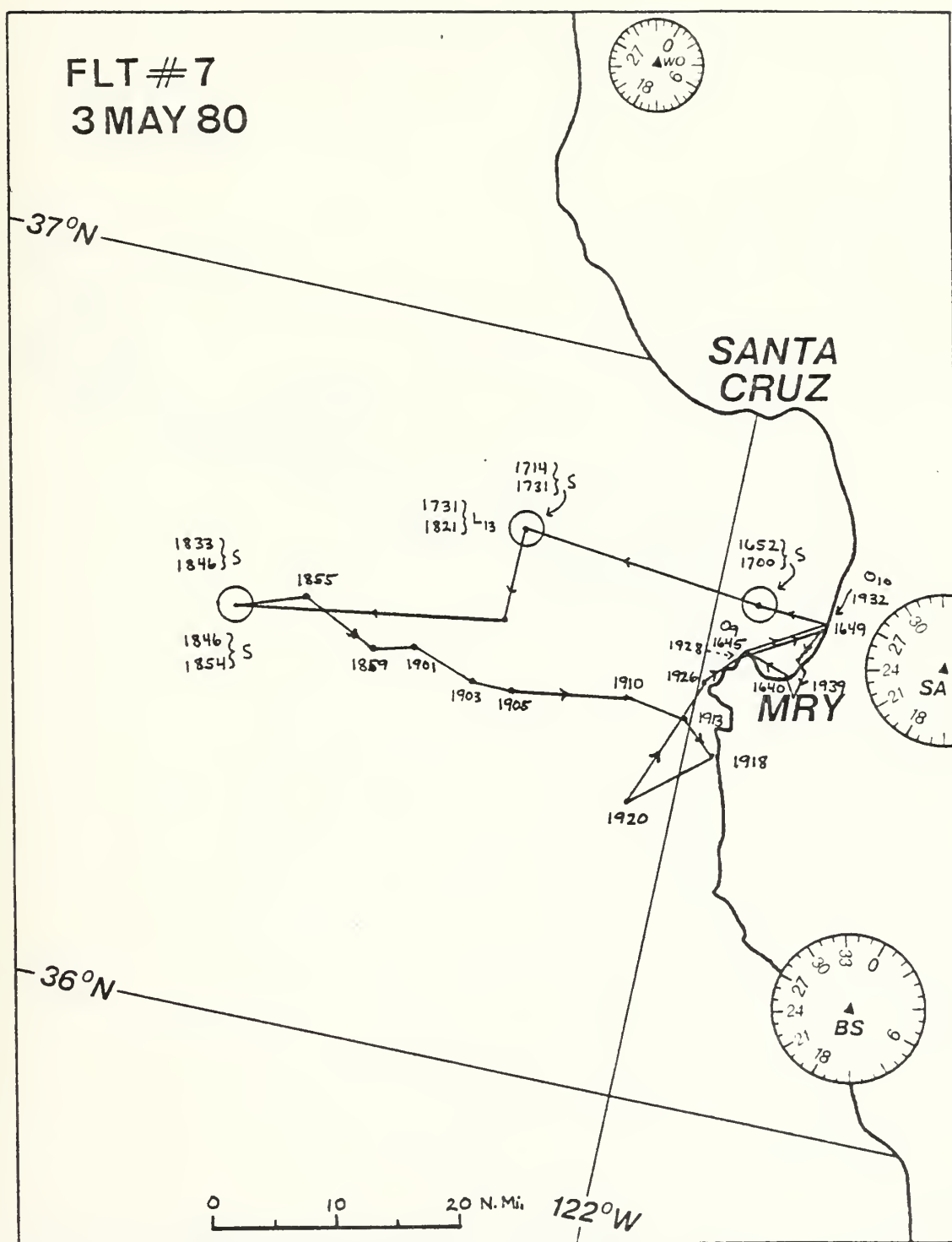


Figure 3.12 Same as figure 3.11 except afternoon of 3 May, 1980.

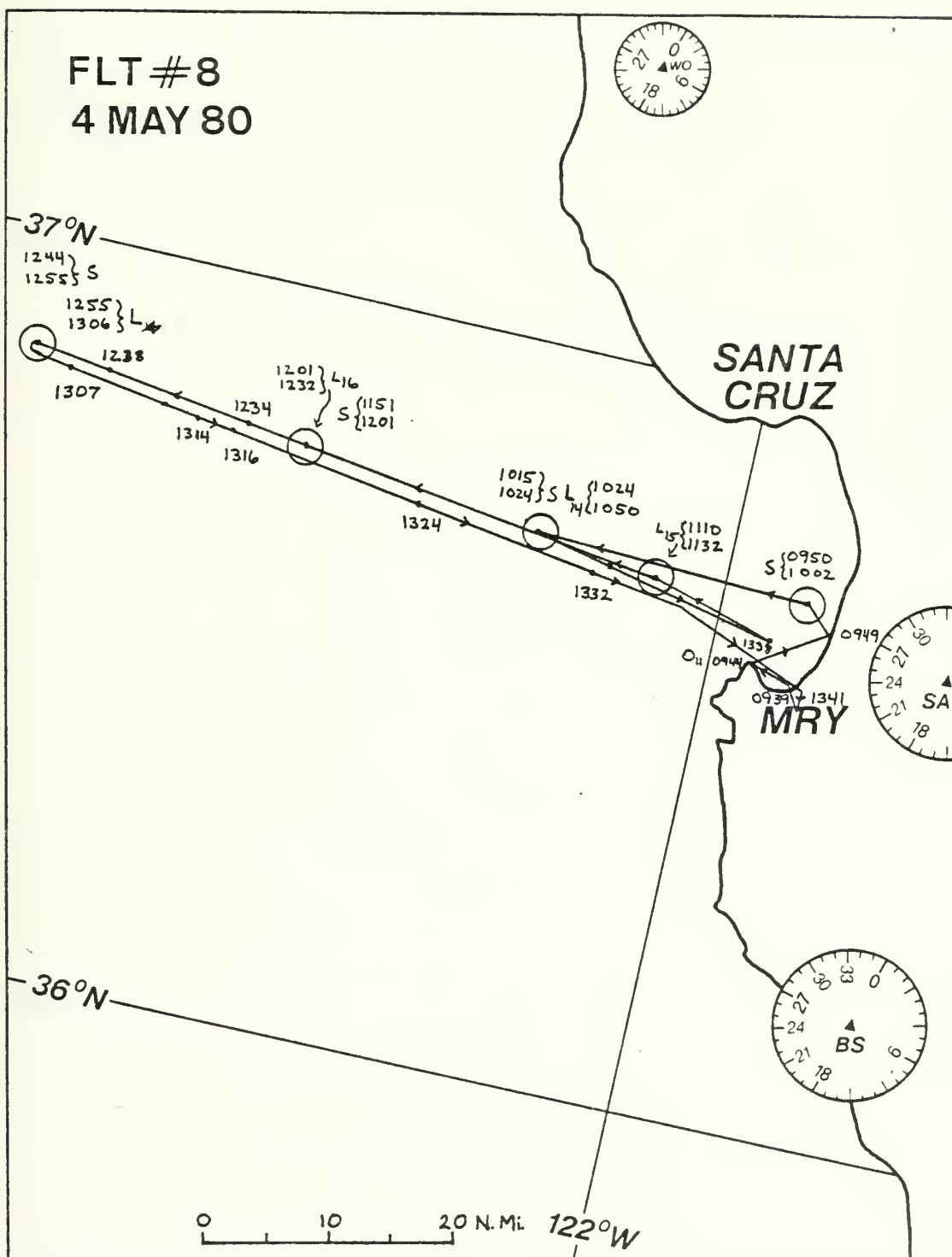


Figure 3.13 Flight path of aircraft on 4 May 1980.

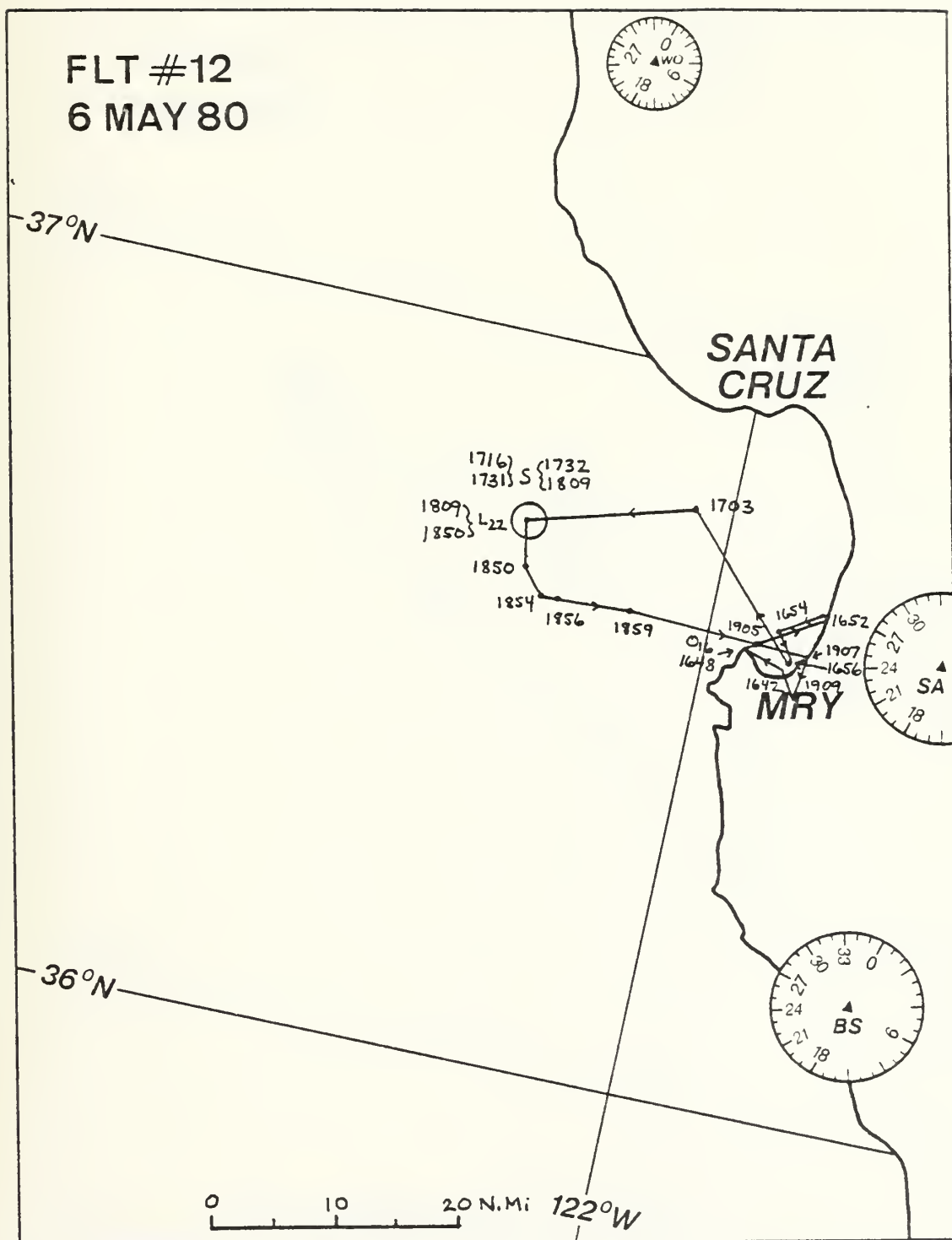


Figure 3.14 Same as figure 3.13 except 6 May, 1980.

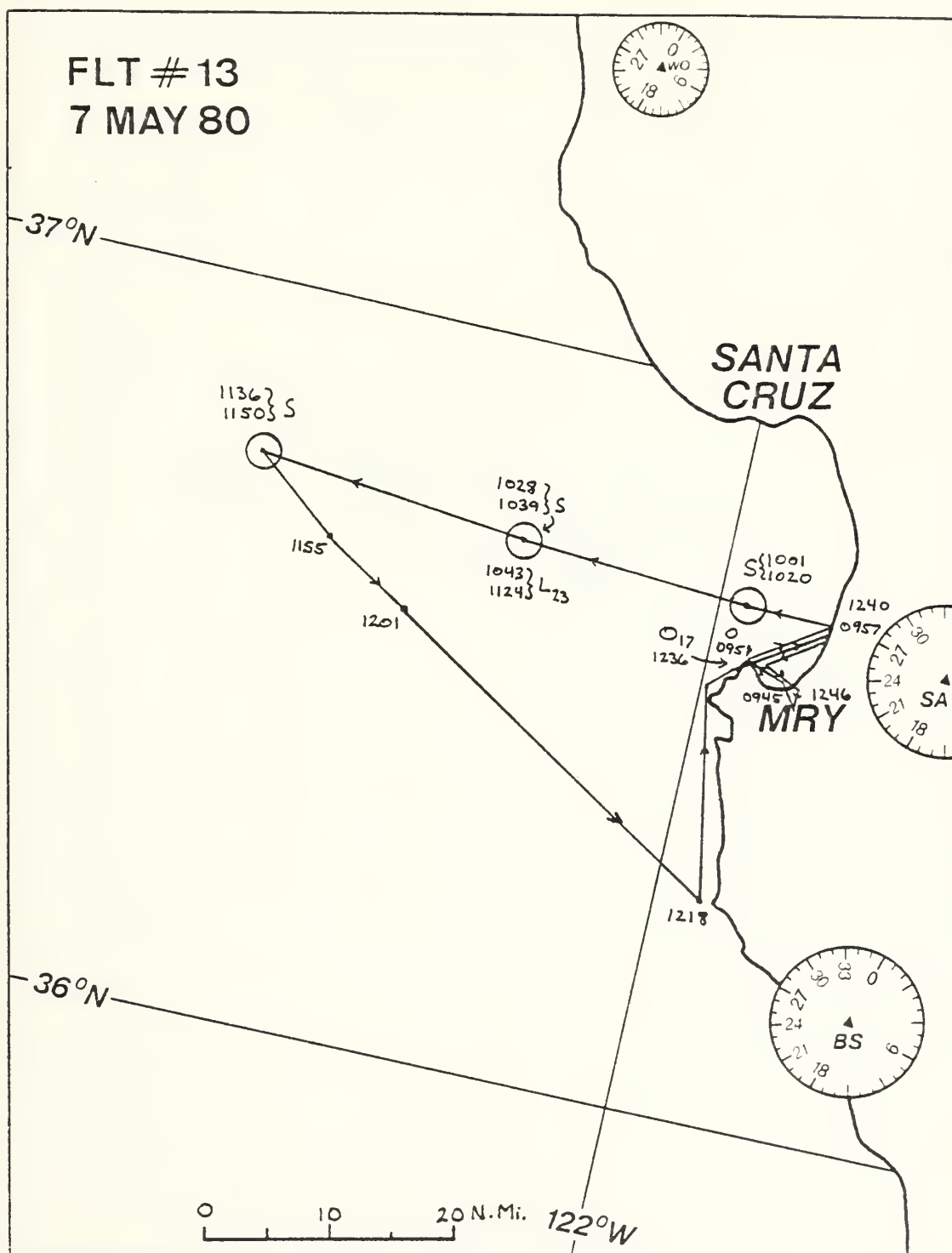


Figure 3.15 Same as figure 3.13 except morning of 7 May 1980.

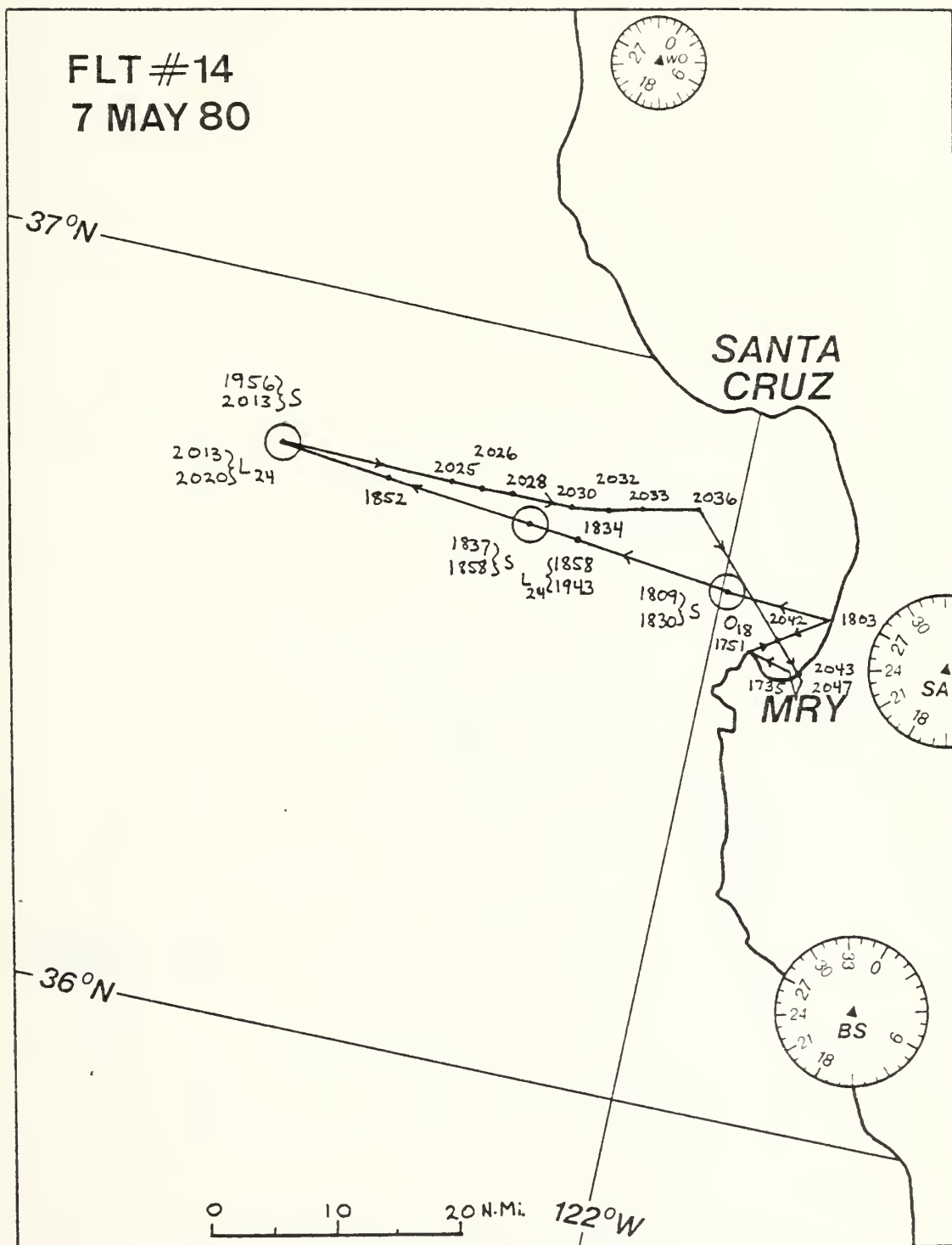


Figure 3.16 Same as figure 3.13 except afternoon of 7 May 1980.

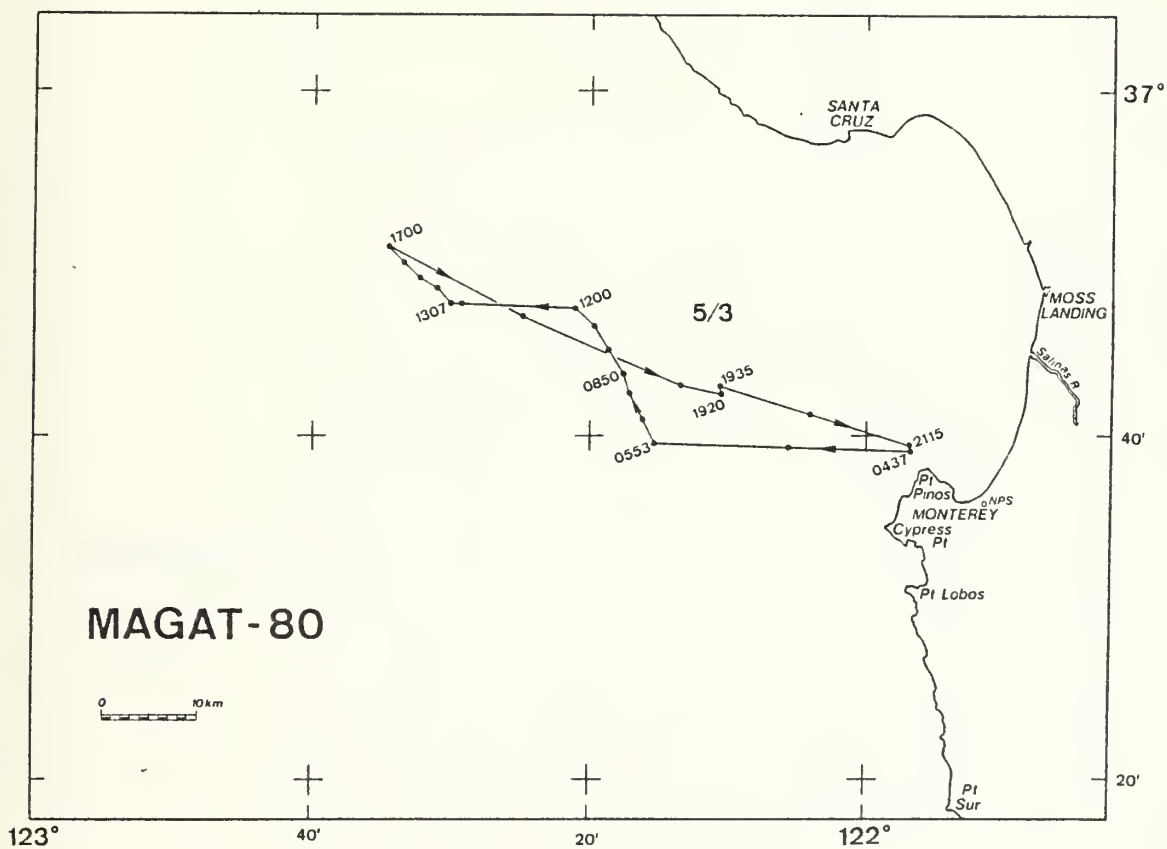


Figure 3.17 Cruise track of R/V ACANIA 3 May 1980.

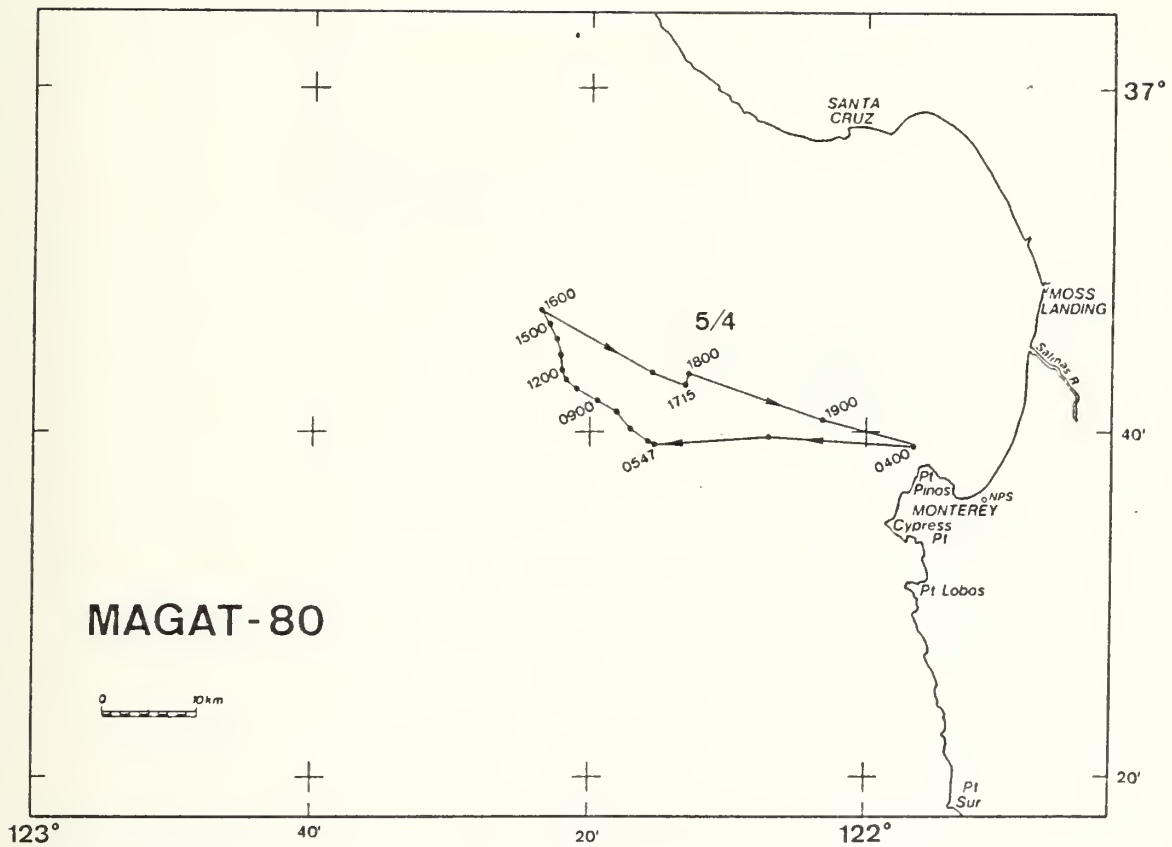


Figure 3.18 Same as figure 3.16 except 4 May 1980.

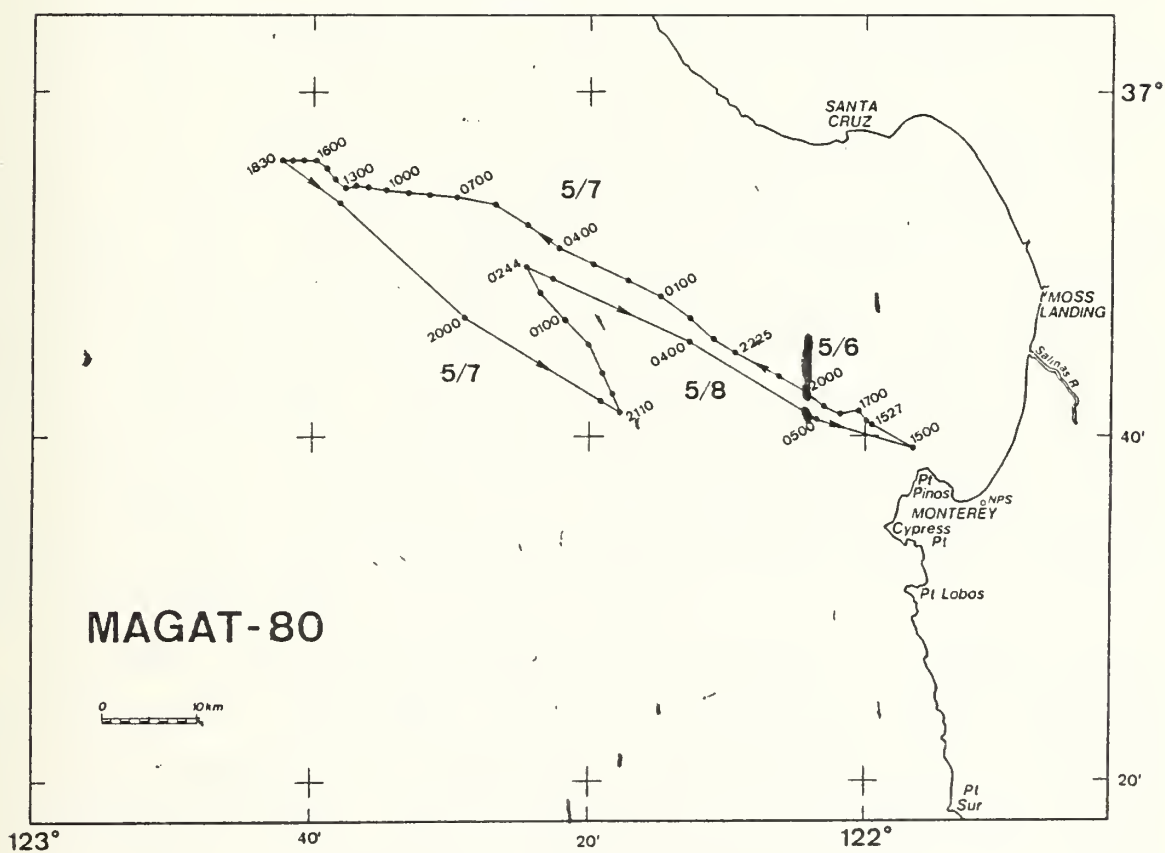


Figure 3.19 Same as figure 3.16 except 6 and 7 May 1980.

were chosen; 3-4 May and 6-7 May. Figures 3.11 through 3.16 indicate the routing of the aircraft flights for the two time blocks, and figures 3.17 through 3.19 depict the course of the R/V ACANIA during the same times.

Atmospheric data from the aircraft soundings were used instead of the radiosondes from the R/V ACANIA. This was done for two reasons: first because the aircraft soundings contained more levels, and second they were in closer proximity to the aircraft aerosol ladders. Atmospheric and aerosol data for the first run was taken from flight 6, on the morning of 3 May. The locations and times are shown in figure 3.9. The aircraft was approximately 45 miles from the coast when a sounding was taken at 1143 PDT, and an aerosol ladder (111) was taken at 1200 PDT. Data for the two verifications of atmospheric parameters and aerosol values were chosen based on their proximity to the initial data. A sounding and aerosol ladder on the afternoon of 3 May (sounding time of 1714 PDT, and aerosol ladder 113) approximately eight hours from the initial time was chosen for the first verification, and is depicted in the route of flight 7, figure 3.10. Data for the second verification was chosen from flight 8, figure 3.11; sounding time 1151 PDT, and aerosol ladder 116. Data for the two verifications are both within 20 miles of the initial data.

Data for the second model run is shown in figures 3-12 through 3-14. The model was initialized with data from the 1732 PDT sounding and ladder 122, approximately 25 miles off the Monterey coast. The first verification data was taken from flight 12 the next morning approximately 17 hours later; sounding time 1743 PDT and ladder 123. The second verification data was taken from flight 13, approximately 24 hours from the initial data; sounding time 1836 PDT and ladder 124. Data collected for the two verifications were within 5 miles of the location of the initial data.

Additional wind speed, direction, and SST collected from the R/V ACANIA were used for initialization and verification of the two model runs. As mentioned in the model description, up to 10 forecast values for each can be input into the model. However, due to the continuous movement of the R/V ACANIA during the MAGAT experiment, where SST values were changing because of strong coastal gradients, a single value of SST was used. This value was chosen when the R/V ACANIA was closest to the areas where the aircraft data was taken for each of the two initialization sites. The wind speed and direction data from the R/V ACANIA was considered representative of the data collection sites, and therefore input into the model runs at approximately 3 hour intervals.

IV. MODEL INITIALIZATION AND RESULTS

A. DIGITIZED ATMOSPHERIC SOUNDINGS

The atmospheric inputs for the model (chapter 2) are:

1. The mixed layer equivalent potential temperature (C) and specific humidity (gm/kg).
2. The "jump" discontinuities in each of the above values. The jump meaning the difference between the mixed layer value and the value at the top of the inversion.
3. The lapse rate for each parameter value above the inversion.
4. The depth of the well mixed-layer.

To simplify the process of calculating these values from the soundings, a digitizing scheme was designed by the Environmental Physics Group at the Naval Postgraduate School. This scheme transforms the sounding into the structure that describes the necessary model inputs. Examples are shown in figures 4.1 and 4.2. Note that the "jumps" are depicted as occurring in an infinitely thin layer.

B. ADDITIONAL MODEL INPUT AND ADJUSTMENTS TO THE DIGITIZED SOUNDINGS

The reason for making adjustments to the atmospheric part of the model is to provide a better basis for evaluating the behavior of the aerosol prediction. This is optimized when the model is producing the best possible forecast of the atmospheric parameters. The parameters are forecast very well in both model runs, with these adjustments made. The model is accurately describing the height of the inversion through adjustments in the subsidence rate, and the lifting condensation level (ICL) is accurately generating clouds

through adjustments to the temperature and specific humidity which are within the limits of instrumentation error. The cloud verifications were made with satellite data and observations from the R/V ACANIA log.

An initial input for the model is the subsidence rate. Using a first guess of -0.005 m/sec, the model generated a plot of the inversion height for the 24-hour period. Based on the verification data, the subsidence rate was further adjusted to bring both the predicted and observed inversion height values together. Then a small adjustment was made to the mixed layer values to match the stability and cloud/cloud free patterns with what was actually observed during the period. In the first model run (3 May), the potential temperature was increased 0.5 degrees and the specific humidity was decreased 1 gm/kg. The resultant subsidence rate necessary to match the predicted and observed inversion height was -0.0042 m/sec. These adjustments yield an atmospheric profile similar to what was actually observed. The air mass became slowly saturated enough to generate clouds in the upper part of the mixed layer at about 0300 PDT on 4 May. Plots of the inversion and LCL behavior, and the temperature and humidity profiles are shown in figure 4.3. In the plot for LCL and inversion height, the letter "H" depicts the verification times and values for the inversion height, and the letter "L" similarly indicates values for the LCL verifications. The letters "T" and "Q" in the temperature and specific humidity graphs indicate verification values for each respective value.

The atmospheric plots for the second model run (6 May) are seen in figure 4.4. For this run the specific humidity was reduced from 6.48 to 6.3 gm/kg, the potential temperature was unchanged, and a subsidence rate of -0.01 m/sec was input for the run.

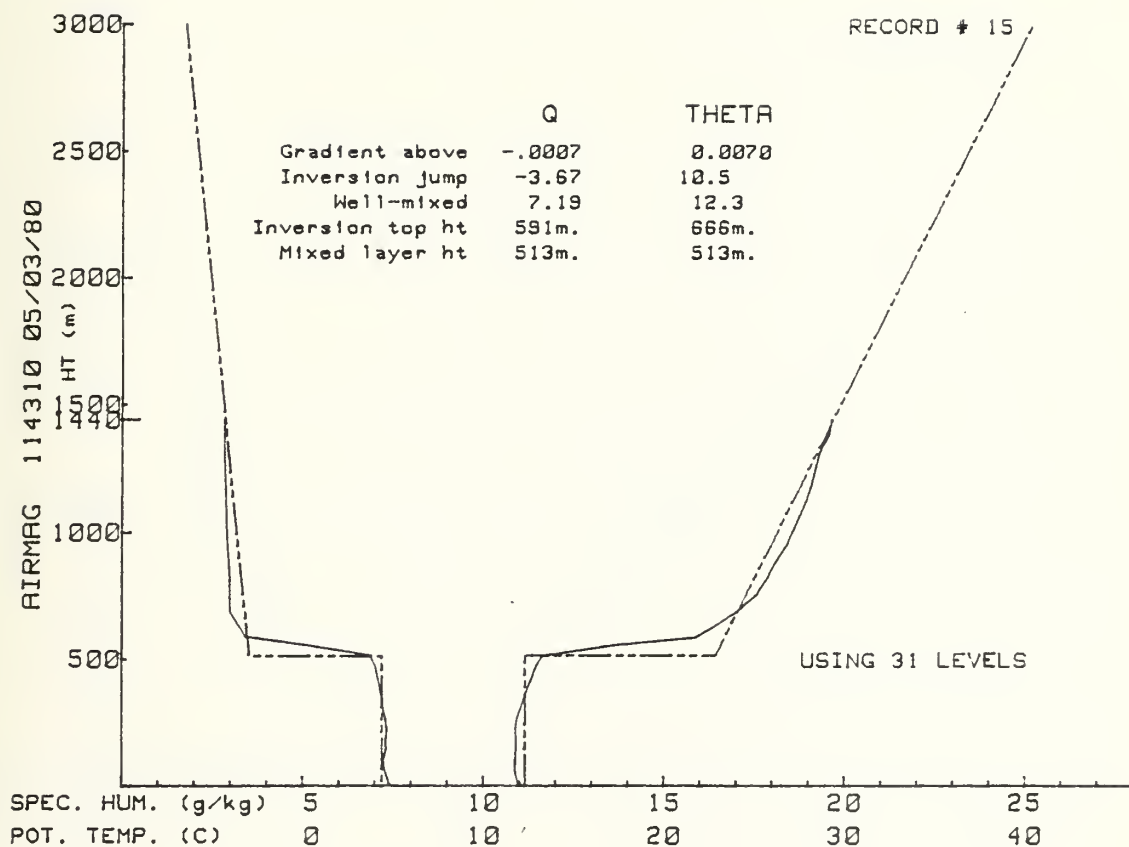


Figure 4.1 Digitized sounding for first model run,
3 May 1980, 1143 PDT.

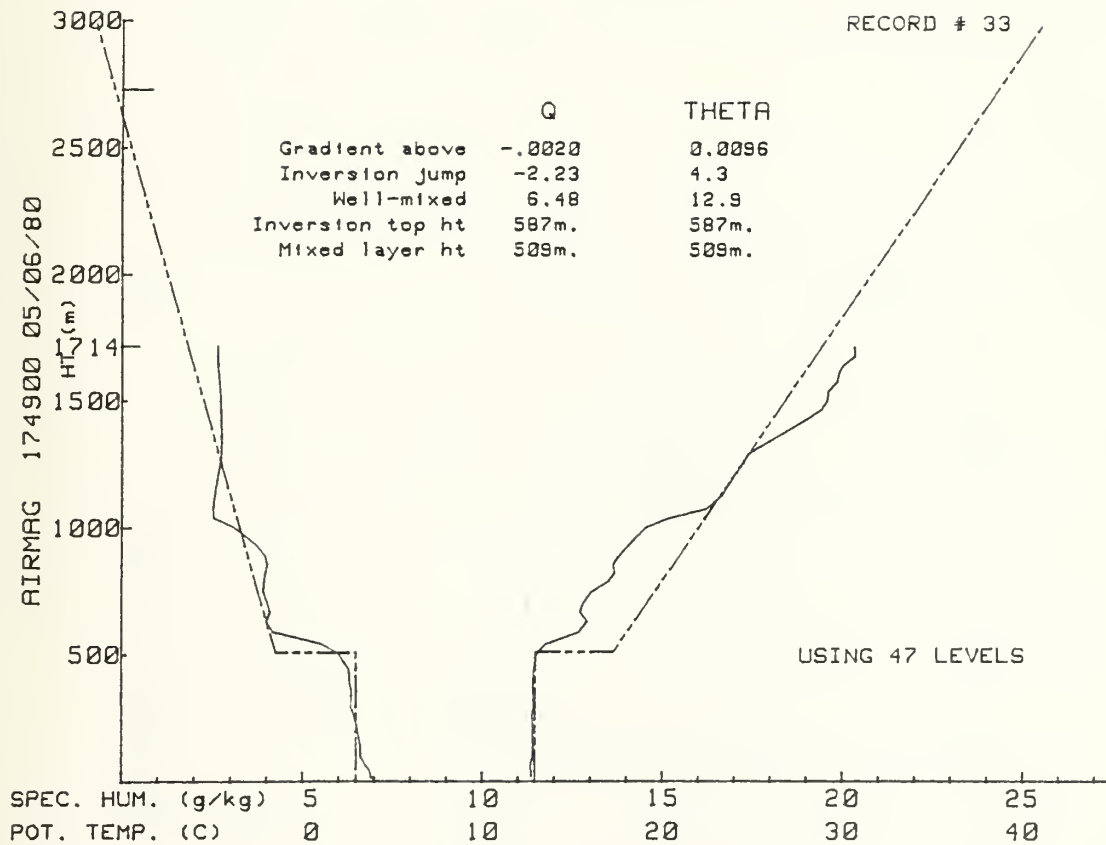


Figure 4.2 Same as figure 4.2, except for second run,
6 May 1980, 1749 PDT.

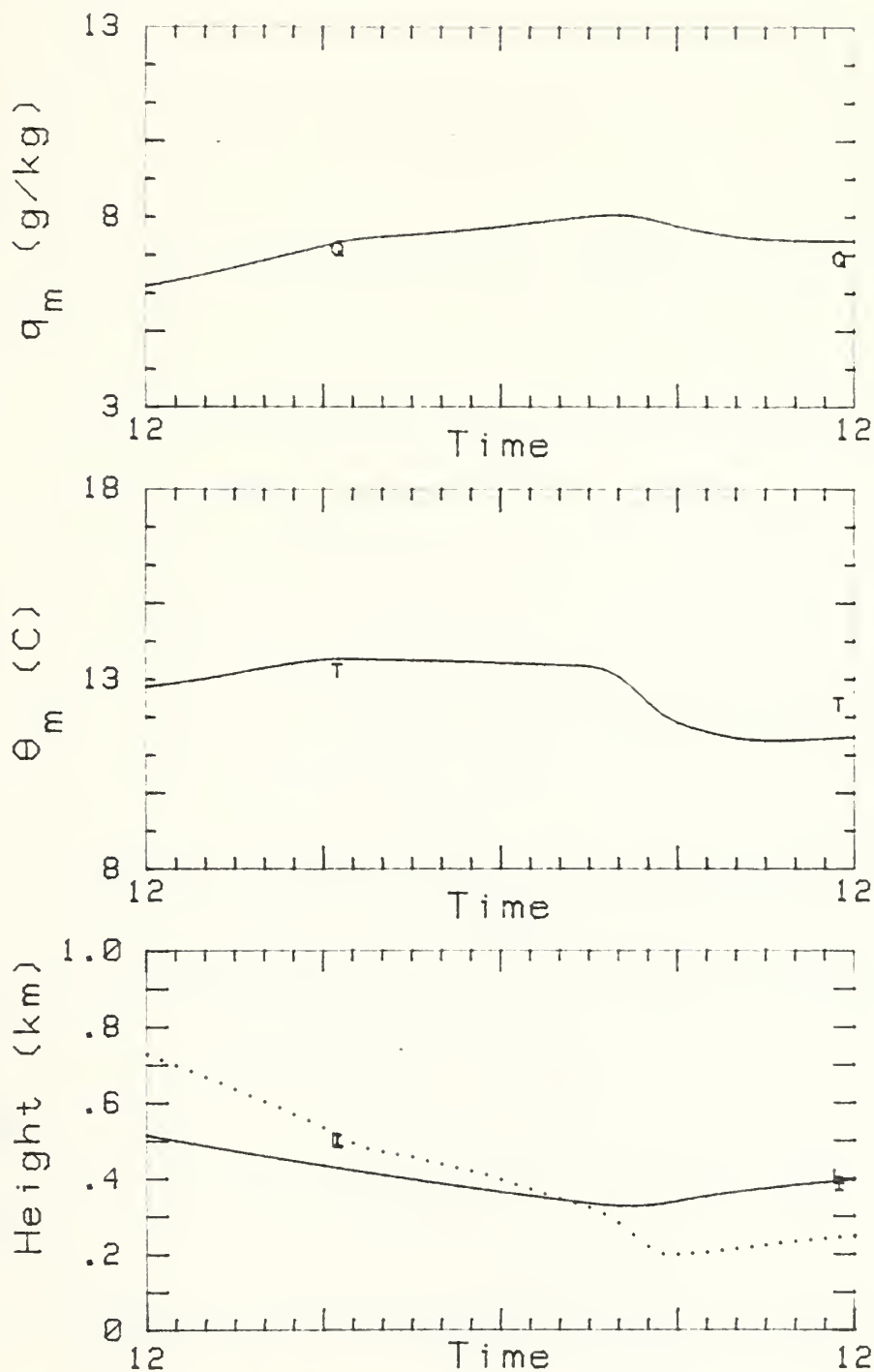


Figure 4.3 Plots of inversion and LCL heights, temperature, and humidity profiles, first run.

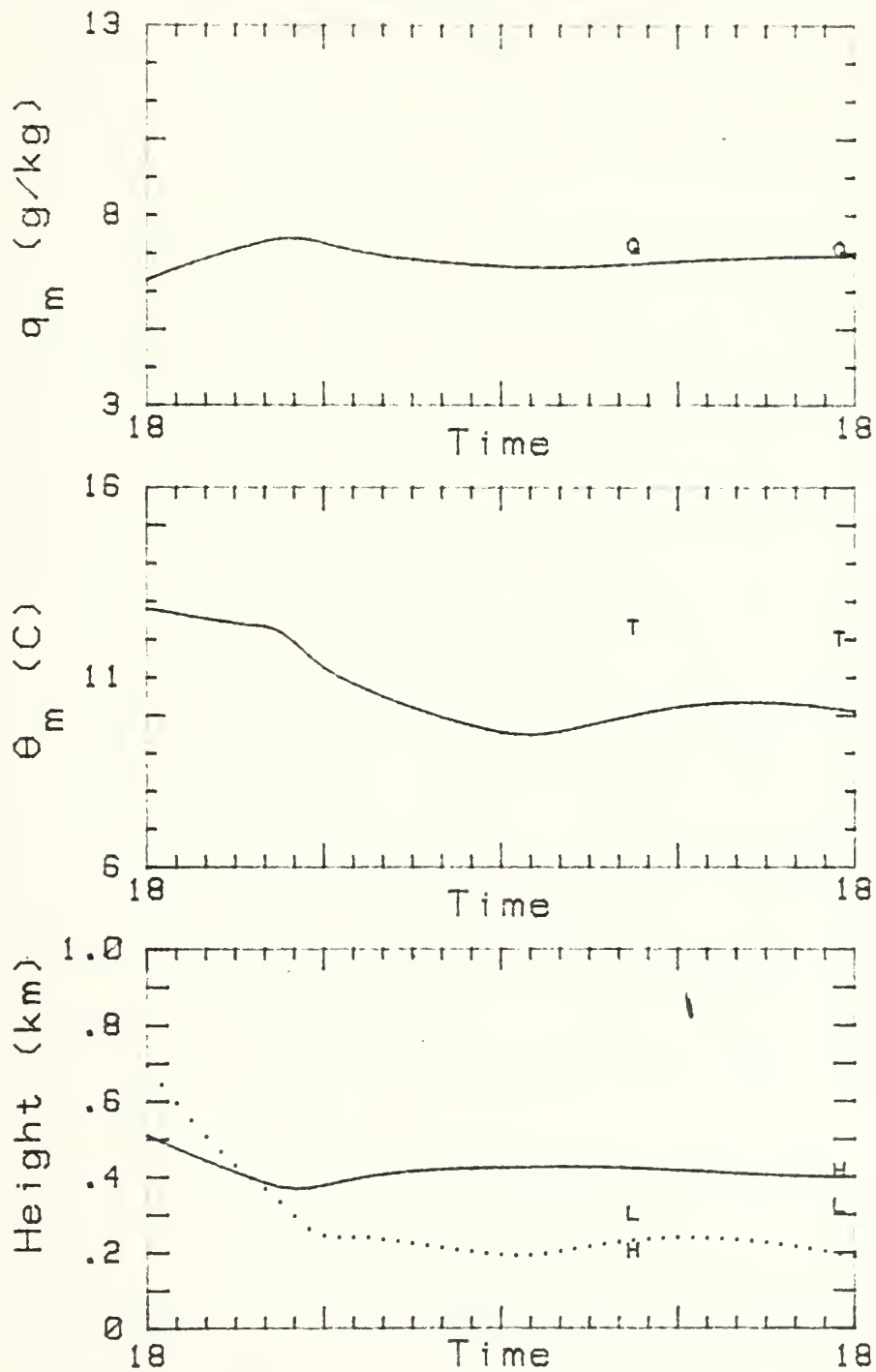


Figure 4.4 Same as Figure 4.3, except for second run.

C. AEROSOL INITIALIZATION PROCEDURES

The aerosol data were gathered in ladders, usually up to five kilometers, and were of actual concentrations of particles for a given increment of radius, $n(r)$. This number contained both marine and continental components, collected at the ambient relative humidity.

The initialization scheme was performed in three main steps. The first step was to identify the marine and continental components. By using the digitized soundings for each model run, a determination was made of two height values: one representing the well mixed-layer and the other representing the free troposphere, above the inversion. Both the mixed layer and free troposphere aerosol counts for each of the five radii were calculated. The second step was to apply the humidity growth factor to the values and calculate dv/dr . The relationship between $n(r)$, which was measured, and dv/dr is given by equation 2-2. The final step was to subtract, for each radius, the free troposphere dv/dr value from the mixed layer dv/dr value. With the assumption of a constant profile of continental aerosols through both the mixed layer and into the free troposphere, this subtraction leaves in only the mixed layer marine components, normalized to 80 percent relative humidity. The values of dv/dr used to initialize the model, both equilibrium and MAGAT, are shown in tables 4.1 and 4.2.

This three step process was done for both model runs, and for two verification times within each run. As described in chapter III, the verification ladders were chosen to be as close as possible to the position of the initial aerosol data. In both cases, the verification data were within 15 miles of the initial data. The plots of the aerosol output,

both for the MAGAT and equilibrium initializations, is depicted as $\log_{10} (dv/dr)$ against the 24 hour time period, in half hour time steps. In both (initialization) cases, the "x" values represent the MAGAT verification values. In both model runs, aerosol output for the MAGAT initialization scheme is represented by a continuous line, and the dashed line depicts the run for the equilibrium initialized cases.

TABLE I
Initial equilibrium aerosol values

		radius, μm			
		0.8	2.0	5.0	10
w	6.0	2.8	3.4	3.0	0.3
i	9.0	10	10	5.0	1.0
n	11	18	25	13	6.4
d	13	20	30	15	15
	15	33	22	22	22
π/s	18	28	35	28	28

TABLE II
Initial observed aerosol values

		radius, μm			
		0.8	2.0	5.0	10
3 May run		42.2	21.8	2.8	0
6 May run		45.4	22.8	5.2	5.1

When considering the equilibrium initial values from table one, it is easy to see the relationship between wind speed and production. In almost all cases, the aerosol volume counts increase as the wind speed increases. The distribution of radii for a given wind speed, however, is not as well defined. For lower wind speeds, the larger radii are few in number, and as the wind speed increases there is a dramatic increase in the number of larger particles. This is reasonable due to white cap production. Also, there appears to be a slight maximum of particles at 2.0 microns, regardless of wind speed. The 15 micron initialization values in the tables and the model output for the same size are not shown. This is because the observed initial values collected from the aircraft were zero.

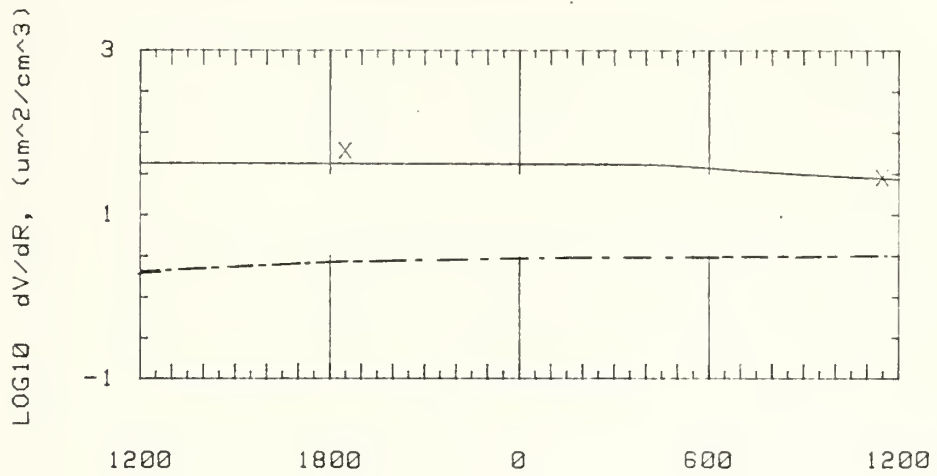
In comparing the MAGAT initial values, one finds that the smaller radii are approximately twice the equilibrium count for even the largest wind speed. It is interesting to note that for such a large variation in initial wind speed for the two days, there is very little variation in the initial values, for all the the particle sizes. Based on results of Monahan [et al 1983], it was also surprising to find no volume counts for the larger particle sizes since wind speed was above 10 m/sec. For the strong wind case, there were no aerosols above 10 microns collected from the aircraft.

D. FIRST MODEL RUN RESULTS

The plots of dv/dr over the 24 hour period for the first model run are shown in figures 4.5 and 4.6. For each radius, the solid line indicates the profile with the MAGAT initialized values, and the dashed line represents the profile with the equilibrium initialization.

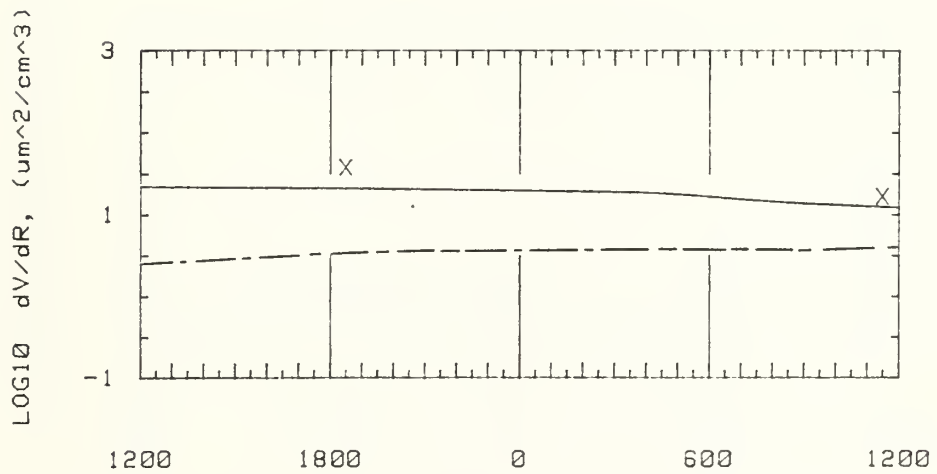
For the three smaller sizes, the model shows little change over the period, however the model does produce a trend in aerosol production. Whatever volumes were used to initialize, the number tends to stay within one order of magnitude over the period. The verification values compare very well to the model run with the MAGAT initialization. The model and verification dv/dr values differ by less than 10 units. For the larger size, 10 microns, note the quick production of aerosol when initialized with a zero value. Within four hours, the model is producing close to the same values as the equilibrium case. From this four-hour point, the two cases behave very much the same. There is a diurnal variation evident in the larger size cases; a lag is noticeable in the production through the night time, with an increase after sunrise and through the morning. The verification values for these larger sizes are not good for either verification scheme.

For RADIUS= .8 um



(a)

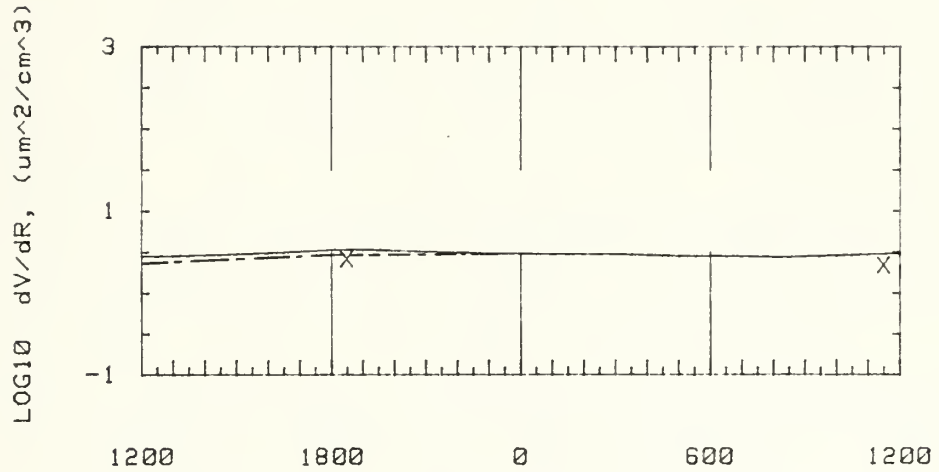
For RADIUS= 2 um



(b)

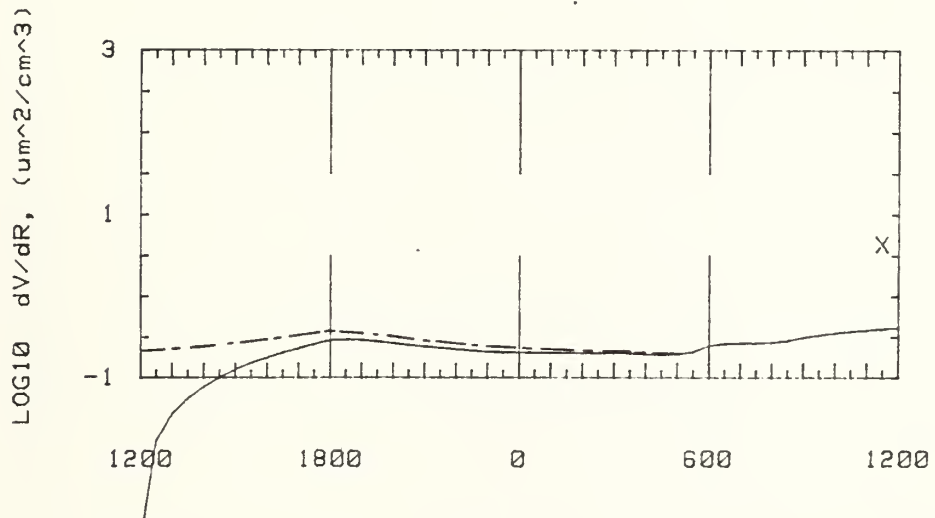
Figure 4.5 Aerosol plots for first run, with a) $r = 0.8 \text{ um}$, and b) $r = 2.0 \text{ um}$.

For RADIUS= 5 um



(a)

For RADIUS= 10 um



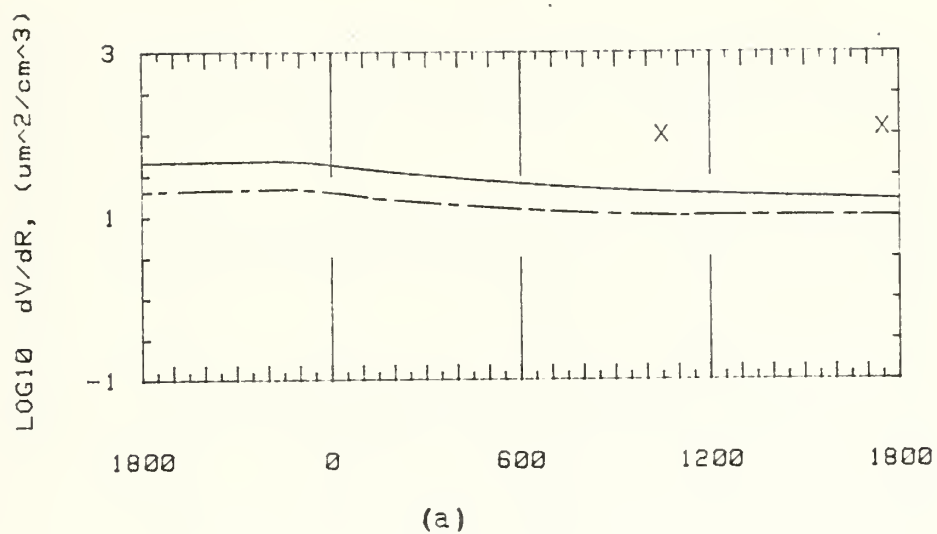
(b)

Figure 4.6 Same as figure 4.5, except a) $r = 5.0 \text{ um}$, and b) $r = 10 \text{ um}$.

E. SECCND MODEL RUN RESULTS

Aerosol plots for both the equilibrium and MAGAT initialization schemes are shown in figure 4.7 and 4.8. The dv/dr values for both schemes are higher, due mainly to the increased wind speed. For all of the particle sizes, there is more of a diurnal variation. This is slightly evident in the smaller radii, and well defined in the larger radii. This variation is strengthened by a wind speed minimum just before sunrise. Note also that the drop in production of all the radii around 0000 PDT coincides with both the slight drop in wind speed from 10 to 8 m/sec, and the formation of clouds, evident in the LCL and inversion figure. This decrease in production due to cloud formation is not noticeable in the first model run. The two initialization schemes are in more agreement than with the first run, again due mainly to the higher wind. With the larger wind speeds in this run, the model is generating values closer to the verification values (in both initialization schemes) than in the first run, where the wind speed is significantly less.

For RADIUS= .8 um



For RADIUS= 2 um

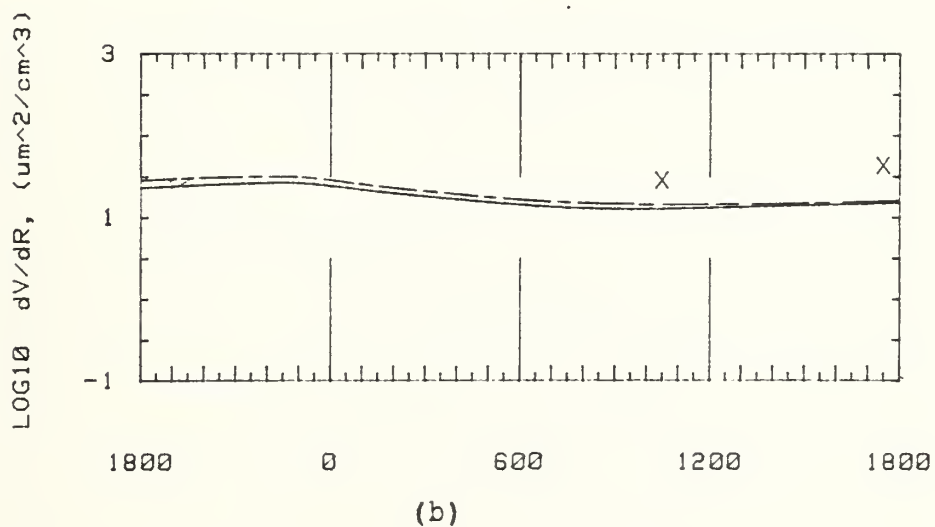
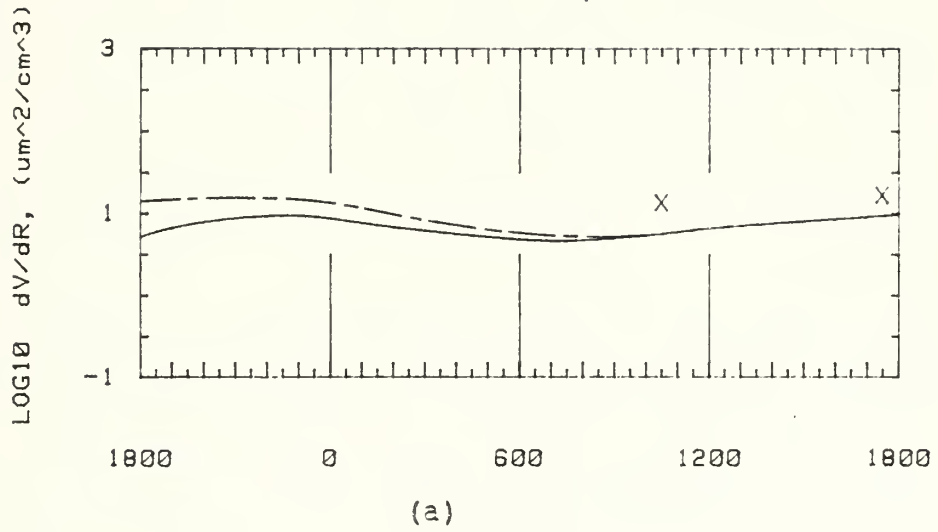


Figure 4.7 Aerosol plots for second run, a) $r = 0.8 \text{ um}$, and
b) $r = 2.0 \text{ um}$.

For RADIUS= 5 um



For RADIUS= 10 um

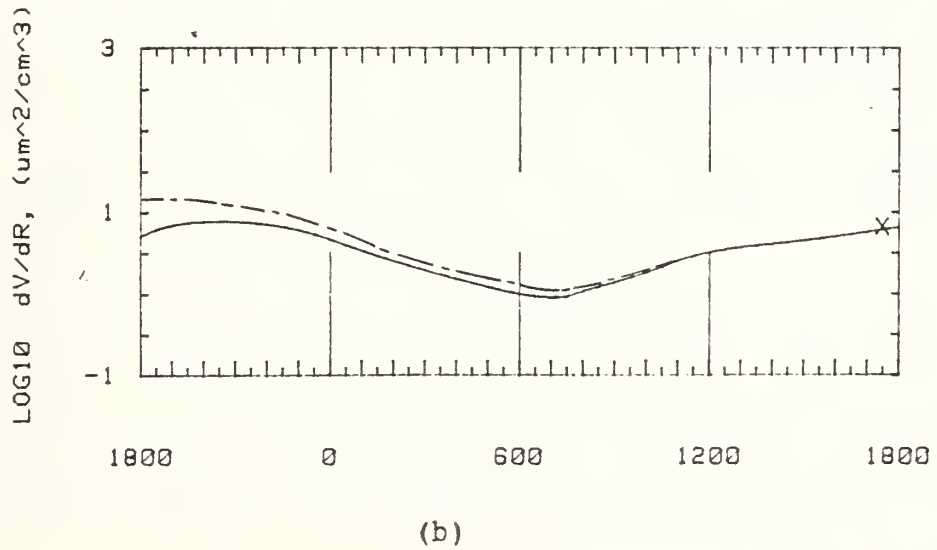


Figure 4.8 Same as figure 4.7, except a) $r = 5.0 \mu\text{m}$ and
b) $r = 10 \mu\text{m}$.

F. SUMMARY OF RESULTS

The model is producing, with a minimum of adjustment, an accurate description of the atmospheric boundary layer parameters. Once a subsidence rate is selected such that the 24-hour predicted inversion height approaches the observed value, the values of temperature and humidity only require a minimum of adjustment. In both cases the verification values of temperature were within 2°C , and the values of specific humidity within 1 gm/kg . More significantly, the trends over the 24-hour periods for both temperature and humidity were accurately described by the model, as defined by the verification data.

With respect to the aerosol input, the model is also producing the correct trend in behavior. There is evidence in the output for the trend in aerosol production to be a function of not only wind speed and relative humidity, but also the concentration of the initial aerosol values. This is seen in the first run, particle sizes 0.8 and 2.0 microns. The atmospheric parameters are the same in both cases, for each radius; but it is the initialization scheme that generates a different trend in each case. The model run with the MAGAT initial values produces a loss in production, and the verification values are within one order of magnitude of the model values. With the equilibrium case, the trend is an increase in production over the time period, with the model verification values two orders of magnitude away from the observed verification values.

The production trends in the second model run, with both initialization schemes, are much the same. In this case there is less of a difference between the model verification values for the two initializations. With the exception of the smallest radius, 0.8 microns, the verification values

for all the radii of the second run are within one order of magnitude of the model output. The fact that the MAGAT initial values are closer to an equilibrium value at a higher wind speed seems to imply a less sensitive model, when initialized with a higher wind speed. Accordingly, aerosol production is high; and the model accurately predicts the behavior of the aerosol in the stronger wind case.

V. CONCIUSIONS

The boundary layer model, with a minimum of input, will produce an accurate description of the MABL [Davidson et al, 1984] and the aerosol behavior within the marine boundary layer. The model is generating values for marine particles within this layer, and whenever there is a large difference between the predicted and observed values, it was the observed values that were too high. This observation suggests that the observed values collected by the aircraft (made up of marine and continental particles) may have included more continental than originally expected. A linear distribution (vertically, through the boundary layer) was assumed in the aerosol initialization process.

More significantly, the model is correctly identifying the production trend of aerosols over the time period. The model is run with identical atmospheric inputs, and different aerosol initialization schemes produce two different production trends. The wind speed and relative humidity (the only atmospheric inputs of previous models) are the same, and the model is generating different profiles based on initial aerosol concentrations. With a minimum of two case studies, it is clear that the process of entrainment of air from above the mixed layer, containing no marine particles, is affecting the behavior of the model output.

LIST OF REFERENCES

- Barnhardt, E.A. and J.L. Streete, 1970: A Method for Predicting Atmospheric Aerosol Scattering Coefficients in the Infared. J. Appl. Opt., 9, 1337-1344.
- Cottrell, F. G., P. H. Try, P. E. Hodges, and R. F. Wactmann, 1979: ELECTRO-OPTICAL HANDBOOK, Volume I: Weather Support for Precision Guided Munitions. Air Weather Service Report AWS/TR-79/002, Scott AFB, IL, 97 pp.
- Davidson, K. L., C. W. Fairall, P. Jones Boyle and G. E. Schacher, 1984: "Verification of an Atmospheric Mixed Layer Model for a Coastal Region," J. Climate and Appl. Meteor., (in press).
- Fairall, C. W., 1980: Atmospheric Optical Propagation Comparisons During MAGAT-80. The BDM Corporation Report BDM/M-010-80, Monterey, Ca, 142 pp.
- , G. E. Schacher, and K. L. Davidson, 1980: Atmospheric Optical Propagation Comparisons During MAGAT-80. Naval Postgraduate School Report NPS-61-81-002, Monterey, Ca., 33 pp.
- , K. L. Davidson and G. E. Schacher, 1982a: Meteorological Models for Optical Properties in the Marine Atmospheric Boundary Layer. Optl. Enginrg., 21, 847-857.
- 1982b: An Analysis of the Surface Production of Sea-Salt Aerosols. Tellus, to appear.

- Monahan, E. C., C. W. Fairall, K. L. Davidson and P. A. Jones, 1983: "Observed Inter-Relationships amongst 10 m-Elevation Winds, Oceanic Whitecaps and Marine Aerosol," Quart. J. Roy. Meteor. Soc., 109, 379-392.
- Wells, W. C., G. Gal and M. W. Munn, 1977: Aerosol Distributions in Maritime Air and Predicted Scattering Coefficients in the Infrared. J. Appl Opt., 16, 654-659.
- Wu, J., 1979: Spray in the Atmospheric Surface Layer: Review and Analysis of Laboratory and Oceanic Results. J. Geophys. Res., 84, 1693-1704.

INITIAL DISTRIBUTION LIST

	No. Copies
1. Defense Technical Information Center Cameron Station Alexandria, Virginia 22314	2
2. Library, Code 0142 Naval Postgraduate School Monterey, California 93943	2
3. Commander Naval Oceanography Command NSII Station, Mississippi 39529	1
4. Commanding Officer Fleet Numerical Oceanography Center Monterey, California 93940	1
5. Officer-in-Charge Naval Environmental Prediction Research Facility Monterey, California 93940	1
6. Prof. R. J. Renard, Code 63Rd Naval Postgraduate School Monterey, California 93943	1
7. Prof. C. N. K. Mooers, Code 68Mr Naval Postgraduate School Monterey, California 93943	1
8. Department of Meteorology Library, Code 63 Naval Postgraduate School Monterey, California 93943	1
9. Major Patrick Herod AFIT/CIRF Wright-Patterson AFB, Ohio 45433	2
10. Air Weather Service Technical Library Scott AFB, Illinois 62225	1
11. Atmospheric Sciences Lab LELAS-AS-P White Sands Missile Range, New Mexico 88002	1
12. Captain David J. Saunders Det 6, 2nd Wea Wng APO New York 09128	1
13. Director of Research and Administration Code 012 Naval Postgraduate School Monterey, California 93943	1
14. Dr. C. W. Fairall Department of Meteorology Walker Building Pennsylvania State University University Park, Pennsylvania 16802	1

15.	Prof. K. L. Davidson, Code 63Ds Naval Postgraduate School Monterey California 93943	10
16.	Prof. G. E. Schacher, Code 61Sq Naval Postgraduate School Monterey California 93943	1
17.	Dr. A. Goroch Naval Environmental Prediction Research Facility Monterey California 93940	
18.	CDR K. Van Sickle Director of Research Naval Environmental Prediction Research Facility Monterey California 93940	1
19.	Dr. Barry Katz Code R42 Naval Surface Weapons Center White Oak Laboratory Silver Spring, Maryland 20362	1
20.	Dr. J. H. Richter Code 532 Naval Oceans Systems Center San Diego, California 92152	1
21.	Dr. Loether Ruhnke Code 8320 Naval Research Laboratory Washington D.C. 20375	1

207730

Thesis

S186 Saunders

c.1 Evaluation of an
aerosol prediction
model for coastal re-
gions using marine
aerosol generation and
transport data.

207730

Thesis

S186 Saunders

c.1 Evaluation of an
aerosol prediction
model for coastal re-
gions using marine
aerosol generation and
transport data.



thesS186

Evaluation of an aerosol prediction mode



3 2768 002 00273 5

DUDLEY KNOX LIBRARY